Molecular phylogenetics and microsatellite analysis reveal a new pathogenic *Ceratocystis* species in the Asian-Australian clade

F. F. Liu[ab], I. Barnes[c], J. Roux[d], M. J. Wingfield[a] and S. F. Chen[ab]*

[a]Department of Microbiology and Plant Pathology, Forestry and Agricultural Biotechnology Institute (FABI), University of Pretoria, Pretoria 0028, South Africa;

[b]China Eucalypt Research Centre (CERC), Chinese Academy of Forestry (CAF), ZhanJiang, 524022, GuangDong Province, China;

[c]Department of Genetics, FABI, University of Pretoria, Pretoria 0028; and

[d]Department of Plant and Soil Sciences, FABI, University of Pretoria, Pretoria 0028, South Africa

* E-mail: shuaifei.chen@gmail.com

Abstract

The ascomycete genus *Ceratocystis* has a broad geographic distribution and includes pathogens of a wide range of mostly woody hosts. Black rot of *Colocasia esculenta* (taro), a popular cultivated root crop in China, is caused by a species of *Ceratocystis* broadly treated as *C. fimbriata sensu lato*. Recently, isolates of *Ceratocystis* were obtained from black rot lesions on *C. esculenta* corms in two Chinese provinces. Sequence comparison of the ITS, partial β-*tubulin*, *TEF-1*α, *MS204* and *RPBII* gene regions were used to identify these isolates and compare them to other *Ceratocystis* species. Furthermore, the diversity of *Ceratocystis* species in the Asian-Australian clade (AAC) was investigated using 23 microsatellite markers. Results showed that the isolates from *C. esculenta* represent a novel species, which is morphologically and phylogenetically different to closely related species in the AAC, and is described here as *Ceratocystis changhui* sp. nov. In microsatellite analyses, this new species also emerged as distinct from others in the AAC. Inoculation tests showed that *C. changhui* sp. nov. is a virulent pathogen of *C. esculenta* corms, but produces only small lesions on *Eucalyptus grandis* and *Eriobotrya japonica*.

Introduction

Species in the Ceratocystidaceae (Microascales, Ascomycota) occur on a wide range of hosts with a broad geographic distribution (De Beer *et al*., 2014). The family encompasses 11 genera, *Ambrosiella*, *Berkeleyomyces*, *Bretziella*, *Ceratocystis*, *Chalaropsis*, *Davidsoniella*, *Endoconidiophora*, *Huntiella*, *Meredithiella*, *Phialophoropsis* and *Thielaviopsis*, which include plant pathogens, insect associates and the causal agents of sap stain in lumber (De Beer *et al*., 2014, 2017; Nel *et al*., 2017). *Ceratocystis* is the largest genus in the family including many important plant pathogens such as those of fruit and forest trees as well as tuber crops (Kile, 1993; Engelbrecht & Harrington, 2005; Roux & Wingfield, 2009; Al Adawi *et al*., 2013). These pathogens cause a wide range of symptoms such as staining of vascular tissues, stem and branch cankers, wilt, and black rot of tubers (Kile, 1993; Roux & Wingfield, 2009). The genus is typified by *C. fimbriata*, which was originally described causing rot of *Ipomoea batatas* (sweet potato; Halsted, 1890).

Ceratocystis species are broadly considered to reside in four well-supported phylogenetic lineages linked to geographic regions. Authors investigating the biogeography of these fungi have used somewhat different notations for these clades (Harrington, 2000; Mbenoun *et al*., 2014; Li *et al*., 2016, 2017). For the present study, the groupings provided by Li *et al*. (2017) are used. Thus, the clade accommodating the type species *C. fimbriata sensu stricto* is referred to as the Latin American clade (LAC) and isolates that form the basis of the present study are the Asian-Australian clade (AAC).

Recent studies based on multigene DNA sequence phylogenies, morphology and ecology have suggested that species concepts in *Ceratocystis* require re-evaluation (De Beer *et al*., 2014; Mbenoun *et al*., 2014; Fourie *et al*., 2015). For example, a recent study by Fourie *et al*. (2015) showed that several cryptic species could be recognized in the LAC. Using the internal transcribed spacer (ITS) gene region, selected as the universal barcoding region for fungal species identification (Schoch *et al*., 2012), is problematic for some species in the LAC and AAC of *Ceratocystis* because different ITS haplotypes can occur in a single *Ceratocystis* isolate (Al Adawi *et al*., 2013; Harrington *et al*., 2014; Fourie *et al*., 2015; Liu *et al*., 2015). Delineation of taxonomic boundaries, particularly for *Ceratocystis* species in the LAC, has differed amongst researchers; some define species specifically based on phylogenetic inference (De Beer *et al*., 2014; Fourie *et al*., 2015), whereas others have applied a broader population-level concept, particularly for *C. fimbriata sensu lato* (Harrington *et al*., 2014; Oliveira *et al*., 2015a).

Taro (*Colocasia esculenta*) belongs to the family Araceae and is a highly polymorphic species (Chair *et al*., 2016). It is a staple food source in many localities in the humid tropics and subtropics and extends to the temperate zones of East Asia, southern Africa, Australia and New Zealand (Chair *et al*., 2016). The tubers of these plants are susceptible to a disease commonly referred to as black rot caused by *Ceratocystis fimbriata s.l*. (Harrington *et al*., 2005; Thorpe *et al*., 2005; Huang *et al*., 2008; Li *et al*., 2017). The first report of a *Ceratocystis* species causing disease on the Araceae was in 1939 when a post-harvest disease on *C. esculenta* was reported from Japan (Shimizu, 1939). There have subsequently been several reports of this disease from many countries of the world including North and South America and South-east Asia (Harrington *et al*., 2005; Thorpe *et al*., 2005; Huang *et al*., 2008; Li *et al*., 2017). A disease similar to black rot also occurs on related tuber crops in the Araceae, such as on species of *Alocasia*, *Syngonium* and *Xanthosoma* (Uchida & Aragaki, 1979; Thorpe *et al*., 2005; Li *et al*., 2017).

There have been many reports of *Ceratocystis* spp. in the LAC causing diseases on several hosts in China. These include black rot on *I. batatas* (Sy, 1956) and *C. esculenta* in YunNan Province (Huang *et al*., 2008), a wilt disease on *Punica granatum* (pomegranate) in YunNan and SiChuan Provinces (Huang *et al*., 2003; Xu *et al*., 2011) and these fungi have also been collected from recently harvested stumps of *Eucalyptus* in GuangDong Province (Chen *et al*., 2013). Black rot on sweet potato is caused by *C. fimbriata s.s*. (Sy, 1956), a pathogen that has been spread globally (Harrington *et al*., 2015). Isolates from *Colocasia* and *Punica* have been treated as *C. fimbriata s.l*. (Harrington *et al*., 2015; Li *et al*., 2016), but have identical ITS sequences to isolates representing a species known as *C. manginecans*, which is a serious tree pathogen in various countries of South-east Asia (Fourie *et al*., 2015, 2016).

There have also been several reports of *Ceratocystis* sp. in the AAC from China. These include *C. cercfabiensis* described from stumps of *Eucalyptus* in FuJian, GuangDong, GuangXi and HaiNan Provinces in southern China (Liu *et al*., 2015), *C. collisensis* from *Cunninghamia lanceolata* in FuJian Province (Liu *et al*., 2015), and isolates representing an undescribed *Ceratocystis* sp. 'Y' (Li *et al*., 2017) from *C. esculenta* (BPI 596161, BPI 596162) imported into the USA from China in 1949 (Thorpe *et al*., 2005; Li *et al*., 2017) and including isolates (C3371–C3376) collected from leaves or twigs of *Eucalyptus* trees in YunNan Province (Li *et al*., 2017). In addition, isolates of *Ceratocystis* from *Eriobotrya japonica* (loquat; E2-2) and *Eucalyptus* (PY1-1, PY2-1) have been reported from YunNan Province in China and broadly treated as *C. fimbriata s.l.* (Li *et al*., 2014a,b). However, the ITS sequences of the latter isolates have 99% similarity to those of *C. uchidae*, a newly described species in the AAC group (Li *et al*., 2017) and 100% similarity to those of the undescribed *Ceratocystis* sp. 'Y' (Li *et al*., 2014a,b).

Recent surveys for *Ceratocystis* species on various plants in China have yielded isolates from *C. esculenta* corms in the YunNan and ShanDong Provinces. Preliminary sequence data, based on ITS sequences, suggested that these isolates are phylogenetically similar to those obtained from *E. japonica* and *Eucalyptus* species in YunNan Province that grouped in the AAC (Li *et al*., 2014a,b, 2017), and also similar to those of the undescribed *Ceratocystis* sp. 'Y' (Li *et al*., 2017). The aim of this study was to identify a collection of isolates from *C. esculenta* in YunNan and ShanDong Provinces, based on phylogenetic analyses of DNA sequences for multiple gene regions and morphological characteristics. Genetic analyses of allele sizes, determined using microsatellite markers, provided deeper, population level information regarding these fungi. The pathogenicity of isolates was tested on corms of *C. esculenta* as well as on stems of *E. japonica* and *Eucalyptus grandis* saplings.

Materials and methods

Fungal isolates

Diseased *C. esculenta* corms were collected at farmer's markets in the YunNan and ShanDong Provinces of China in August 2014 and May 2015, respectively. Ascomata of *Ceratocystis* species were common on the surfaces of wounds (Fig. 1a,b) and in some cases, the entire corms were rotten. Cultures were made by transferring ascospore masses from the tips of the ascomata to 2% malt extract agar (MEA; 20 g malt extract and 20 g agar per litre of water). Cultures were incubated at 25 °C for 4–7 days and then purified by making single hyphal tip transfers to fresh MEA plates.

Figure 1. Disease symptoms caused by *Ceratocystis changhui* on *Colocasia esculenta* (taro) in YunNan Province, China; (a) diseased *C. esculenta* corms with the fungal mycelia growing from rotten sites (shown by arrows); (b) fruiting structures with ascospore masses on the black rot lesion of *C. esculenta*.

All 31 isolates obtained in this study were deposited in the culture collection of the China Eucalypt Research Centre (CERC), Chinese Academy of Forestry (CAF), ZhanJiang, GuangDong Province, China and in the Culture Collection (CMW) of the Forestry and Agricultural Biotechnology Institute (FABI), University of Pretoria, South Africa. Representative isolates of a newly described taxon were deposited with the Westerdijk Fungal Biodiversity Institute (CBS), Utrecht, Netherlands. Dried specimens were deposited with the National Collection of Fungi (PREM), Pretoria, South Africa.

This study also included six *Eucalyptus* isolates (C3371–C3376) of *Ceratocystis* sp. 'Y' (Li *et al*., 2017) supplied by Professor T. Harrington, Department of Plant Pathology and Microbiology, Iowa State University (Tables 1 & S1). In addition, isolates of 11 other *Ceratocystis* species in the AAC were used. These included 40 isolates of *C. cercfabiensis* that were collected previously from *Eucalyptus* trees in five provinces of China (Liu *et al*., 2015), four isolates of *C. collisensis*, and two ex-type isolates of each of nine *Ceratocystis* species (*C. atrox*, *C. corymbiicola*, *C. ficicola*, *C. larium*, *C. obpyriformis*, *C. piriliformis*, *C. polychroma*, *C. polyconidia*, *C. uchidae*; Table S1).

Sequencing and multigene phylogenetic analyses

DNA was extracted from all above-mentioned isolates for further analyses. Cultures from single hyphal tips grown on 2% MEA for 2–3 weeks at 25 °C were used for extraction. Mycelia were scraped from the surfaces of MEA plates using a sterile scalpel and transferred to 2 mL Eppendorf tubes. DNA was extracted using the method described by Möller *et al*. (1992). DNA concentrations were determined using a ND-1000 spectrophotometer (Nano Drop Technologies, Thermo Scientific) and dilutions made to approximately 50 ng μL^{-1}.

The 31 isolates from *C. esculenta* corms collected in the present study and the six isolates of *Ceratocystis* sp. 'Y' from *Eucalyptus* were subjected to PCR amplification and subsequent sequencing of five gene regions. These comprised the ITS regions 1 and 2, including the 5.8S

Table 1 List of Ceratocystis isolates included in this study

Species	CMW no.	CERC no.	Other no.	GenBank accession no.					Host (or substrate)	Collectors	Geographic origin
				ITS	β-*tubulin*	*TEF-1α*	*MS204*	*RPBII*			
C. albifundus	CMW 4068		CBS 128992	DQ520638	EF070429	EF070400	**KY643987**	**KY644041**	*Acacia mearnsii*	J. Roux	South Africa
C. atrox	CMW 19383		CBS 120517	EF070414	EF070430	EF070402	**KY643975**	**KY644029**	*Eucalyptus grandis*	M.J. Wingfield	Australia
C. atrox[T]	CMW 19385		CBS 120518	EF070415	EF070431	EF070403	**KY643976**	**KY644030**	*E. grandis*	M.J. Wingfield	Australia
C. cercfabiensis[T]	CMW 43029	CERC 2170[a]	CBS 139654	KP727592, KP727593, KP727594	KP727618	KP727643	**KY643963**	**KY644016**	*Eucalyptus* sp.	S.F. Chen & F.F. Liu	HaiNan, China
C. cercfabiensis	CMW 42515	CERC 2345[a]	CBS 139655	KP727588	KP727596	KP727621	**KY643965**	**KY644018**	*Eucalyptus* sp.	S.F. Chen & F.F. Liu	GuangXi, China
C. cercfabiensis	CMW 42795	CERC 2687[a]	CBS 139656	KP727583	KP727619	KP727644	**KY643968**	**KY644022**	*Eucalyptus* sp.	S.F. Chen & F.F. Liu	GuangDong, China
C. cercfabiensis	CMW 42512	CERC 2335		KP727583, KP727589, KP727590, KP727591	KP727607	KP727632	**KY643964**	**KY644017**	*Eucalyptus* sp.	S.F. Chen & F.F. Liu	GuangXi, China
C. cercfabiensis	CMW 42736	CERC 2576		KP727583, KP727584, KP727585	KP727600	KP727625	**KY643966**	**KY644019**	*Eucalyptus* sp.	S.F. Chen & F.F. Liu	GuangDong, China
C. cercfabiensis	CMW 42741	CERC 2581		KP727586, KP727588, KP727587	KP727601	KP727626	**KY643967**	**KY644020**	*Eucalyptus* sp.	S.F. Chen & F.F. Liu	GuangDong, China
C. changhui	**CMW 43268**	**CERC 3601**[a]		**KY643883**	**KY643913**	**KY643935**	**KY643956**	**KY644009**	*Colocasia esculenta*	S.F. Chen	YunNan, China
C. changhui	**CMW 43272**	**CERC 3605**[ab]	**CBS 139798**	**KY643886**	**KY643915**	**KY643937**	**KY643958**	**KY644011**	*C. esculenta*	S.F. Chen	YunNan, China
C. changhui	**CMW 43273**	**CERC 3606**[ab]	**CBS 139799**	**KY643889**	**KY643916**	**KY643938**	**KY643959**	**KY644012**	*C. esculenta*	S.F. Chen	YunNan, China
C. changhui	**CMW 43280**	**CERC 3614**[a]		**KY643887**	**KY643918**	**KY643940**	**KY643961**	**KY644014**	*C. esculenta*	S.F. Chen	YunNan, China
C. changhui[T]	**CMW 43281**	**CERC 3615**[ab]	**CBS 139797**	**KY643884**	**KY643919**	**KY643941**	**KY643962**	**KY644015**	*C. esculenta*	S.F. Chen	YunNan, China
C. changhui	**CMW 46111**	**CERC 7516**		**KY643890**	**KY643906**	**KY643928**	**KY643950**	**KY644003**	*C. esculenta*	S.F. Chen	ShanDong, China
C. changhui	**CMW 46112**	**CERC 7527**		**KY643891**	**KY643907**	**KY643929**	**KY643951**	**KY644004**	*C. esculenta*	S.F. Chen	ShanDong, China
C. changhui	**CMW 46113**	**CERC 7530**		**KY643892**	**KY643908**	**KY643930**	**KY643952**	**KY644005**	*C. esculenta*	S.F. Chen	ShanDong, China
C. changhui	**CMW46116**	**CERC 7543**		**KY643895**	**KY643911**	**KY643933**	**KY643954**	**KY644007**	*C. esculenta*	S.F. Chen	ShanDong, China
C. collisensis[T]	CMW 42552	CERC 2459	CBS 139679	KP727578	KP727614	KP727639	**KY643970**	**KY644024**	*Cunninghamia lanceolata*	S.F. Chen & F.F. Liu	FuJian, China
C. collisensis	CMW 42554	CERC 2466	CBS 139647	KP727580	KP727615	KP727640	**KY643972**	**KY644026**	*C. lanceolata*	S.F. Chen & F.F. Liu	FuJian, China
C. corymbiicola[T]	CMW 29120		CBS 127215	HM071902	HM071914	HQ236453	**KY643983**	**KY644037**	*Corymbia variegata*	G.K. Nkuekam	Australia
C. corymbiicola	CMW 29349		CBS 127216	HM071919	HQ236455	HM071905	**KY643984**	**KY644038**	*Eucalyptus pilularis*	G.K. Nkuekam	Australia
C. ficicola[T]	CMW 38543		C1355, BPI 843724	NR_119410	**KY685077**	KY316544	**KY685080**	**KY685082**	*Ficus carica*	Y. Kajitani	Japan
C. ficicola	CMW 38544			**KY685076**	**KY685078**	**KY685079**	**KY685081**	**KY685083**	*F. carica*	Y. Kajitani	Japan
C. fimbriata	CMW 1547		CBS 123010	AF264904	EF070443	EF070395	KJ601577	KJ601613	*Ipomoea batatas*	E.C.H. McKenzie	Papua New Guinea
C. fimbriata	CMW 15049		CBS 141.37	DQ520629	EF070442	EF070394	N/A	N/A	*I. batatas*	C.F. Andrus	USA

Species	CMW no.	CERC no.	Other no.	GenBank accession no.					Host (or substrate)	Collectors	Geographic origin
				ITS	β-*tubulin*	*TEF-1α*	*MS204*	*RPBII*			
C. fimbriata s.l.			PY2-1	KF963101	N/A	N/A	N/A	N/A	*Eriobotrya japonica*	J. Li	YunNan, China
C. fimbriata s.l.			PY1-1	KF963102	N/A	N/A	N/A	N/A	*E. japonica*	J. Li	YunNan, China
C. fimbriata s.l.			E2-2	KJ511481	N/A	N/A	N/A	N/A	*Eucalyptus* sp.	J. Li	YunNan, China
Ceratocystis sp. Y			BPI596161	AY526304	N/A	N/A	N/A	N/A	*C. esculenta*	Li *et al.*	Import from China in 1949
Ceratocystis sp. Y			BPI596162	AY526305	N/A	N/A	N/A	N/A	*C. esculenta*	Li *et al.*	Import from China in 1949
Ceratocystis sp. Y[c]	**CMW 49317**		**E2-1-1, C3371**	**KY643879**	**KY643900**	**KY643922**	**KY643944**	**KY643997**	*Eucalyptus* sp.	Li *et al.*	YunNan, China
Ceratocystis sp. Y[c]	**CMW 49318**		**E2-1-2, C3372**	KY306682	**KY643901**	**KY643923**	**KY643945**	**KY643998**	*Eucalyptus* sp.	Li *et al.*	YunNan, China
Ceratocystis sp. Y[c]	**CMW 49319**		**E2-2-1, C3373**	**KY643880**	**KY643902**	**KY643924**	**KY643946**	**KY643999**	*Eucalyptus* sp.	Li *et al.*	YunNan, China
Ceratocystis sp. Y[c]	**CMW 49320**		**E2-2-2, C3374**	KJ511481	**KY643903**	**KY643925**	**KY643947**	**KY644000**	*Eucalyptus* sp.	Li *et al.*	YunNan, China
Ceratocystis sp. Y[c]	**CMW 49321**		**E2-3-1, C3375**	**KY643881**	**KY643904**	**KY643926**	**KY643948**	**KY644001**	*Eucalyptus* sp.	Li *et al.*	YunNan, China
Ceratocystis sp. Y[c]	**CMW 49322**		**E2-3-2, C3376**	**KY643882**	**KY643905**	**KY643927**	**KY643949**	**KY644002**	*Eucalyptus* sp.	Li *et al.*	YunNan, China
C. larium[T]	CMW 25434		CBS 122512	EU881906	EU881894	EU881900	**KY643981**	**KY644035**	*Styrax benzoin*	M.J. Wingfield	Indonesia
C. larium	CMW 25435		CBS 122606	EU881907	EU881895	EU881901	**KY643982**	**KY644036**	*S. benzoin*	M.J. Wingfield	Indonesia
C. obpyriformis	CMW 23807		CBS 122608	EU245004	EU244976	EU244936	**KY643977**	**KY644031**	*A. mearnsii*	R.N. Heath	South Africa
C. obpyriformis[T]	CMW 23808		CBS 122511	EU245003	EU244975	EU244935	**KY643978**	**KY644032**	*A. mearnsii*	R.N. Heath	South Africa
C. pirilliformis	CMW 6569			AF427104	DQ371652	AY528982	**KY643985**	**KY644039**	*Eucalyptus nitens*	M.J. Wingfield	Australia
C. pirilliformis[T]	CMW 6579		CBS 118128	AF427105	DQ371653	AY528983	KJ601594	KJ601630	*E. nitens*	M.J. Wingfield	Australia
C. polychroma[T]	CMW 11424		CBS 115778	AY528970	AY528966	AY528978	**KY643973**	**KY644027**	*Syzygium aromaticum*	M.J. Wingfield	Indonesia
C. polychroma	CMW 11436		CBS 115777	AY528971	AY528967	AY528979	**KY643974**	**KY644028**	*S. aromaticum*	M.J. Wingfield	Indonesia
C. polyconidia[T]	CMW 23809		CBS 122289	EU245006	EU244978	EU244938	**KY643979**	**KY644033**	*A. mearnsii*	R.N. Heath	South Africa
C. polyconidia	CMW 23818		CBS 122290	EU245007	EU244979	EU244939	**KY643980**	**KY644034**	*A. mearnsii*	R.N. Heath	South Africa
C. uchidae[T]	CMW 48505		CBS 115164, C1714	AY526306	**KY643899**	**KY643921**	**KY643943**	**KY643996**	*C. esculenta*	Li *et al.*	Hawaii, USA
C. uchidae	CMW 48501		CBS 114720, C1715	AY526307	**KY643898**	**KY643920**	**KY643942**	**KY643995**	*C. esculenta*	Li *et al.*	Hawaii, USA
C. uchidae			C1931	AY526308	N/A	HM569618	N/A	N/A	*Xanthosoma sagittifolium*	Li *et al.*	Fiji
Davidsoniella virescens	CMW 11164		CBS 123166	DQ520639	EF070441	EF070413	N/A	N/A	*Fagus americanum*	D. Houston	USA

[T]The type isolate of the species. CMW = Culture collection of the Forestry and Agricultural Biotechnology Institute, University of Pretoria, Pretoria, South Africa; CERC = Culture collection of China Eucalypt Research Centre, Chinese Academy of Forestry, ZhanJiang, GuangDong Province, China; CBS = the Westerdijk Fungal Biodiversity Institute, Utrecht, Netherlands.

Isolates indicated in bold are newly identified and described in this study. GenBank accession numbers indicated in bold were generated in this study.

[a]Isolates used for the pathogenicity tests.

[b]Isolates used for the growth study.

[c]Identified as *C. changhui* in this study.

rRNA gene, partial β-tubulin gene (*BT1*), partial translation elongation factor-1α gene (*TEF-1*α), *MS204* and *RPBII* gene regions. The primers used were ITS1 and ITS4 (White *et al*., 1990) for the ITS region, Bt1a and Bt1b (Glass & Donaldson, 1995; Van Wyk *et al*., 2011; Mbenoun *et al*., 2014) for the *BT1* gene, TEF1F and TEF2R (Jacobs *et al*., 2004) for the *TEF-1*α gene, MS204F.ceratoB and MS204R.ceratoB (Fourie *et al*., 2015) for the *MS204* gene and RPB2-5Fb and RPB2-7Rb (Duong *et al*., 2012) for the *RPBII* gene.

Amplification reactions for the five gene regions were conducted in 25 µL final volumes as described by Liu *et al*. (2015). The PCR programme for amplification of the ITS, *BT1* and *TEF1*-α gene regions was carried out as described by Liu *et al*. (2015). An extended-PCR programme was used for the *RPBII* gene region as follows: 95 °C for 5 min, (95 °C for 30 s, 59 °C for 45 s, 72 °C for 90 s) × 10 cycles, (95 °C for 30 s, 59 °C for 45 s, 72 °C for 90 s + 5 s per cycle increase) × 30 cycles and 60 °C for 35 min. The PCR programme used for the *MS204* gene region included an initial denaturation step at 95 °C for 5 min followed by 35 cycles of 30 s at 95 °C, 45 s at 56 °C and 60 s at 72 °C, and a final extension step at 72 °C for 10 min.

PCR products were purified by gel filtration through 6% Sephadex G-50 (Sigma). Sequencing reactions were conducted using both the forward and reverse primers for each gene region using the ABI PRISM BigDye Terminator Cycle Sequencing Ready Reaction kit v. 3.1 (Applied BioSystems). An ABI PRISM 3100 Autosequencer (Applied BioSystems) was used to generate the sequences.

Raw sequence data were edited and assembled using geneious v. 7.0. Preliminary identification was made by submitting sequences to the blast network service of the National Center for Biotechnology Information (NCBI) (http://www.ncbi.nlm.nih.gov) in order to search for closely related species. Preliminary sequence data, based on the ITS sequences, suggested that isolates collected in this study were closely related to *Ceratocystis* species in the AAC. Sequence data for the type strains of *Ceratocystis* species in the AAC were downloaded from GenBank (http://www.ncbi.nlm.nih.gov). Because the sequences for *MS204* and *RPBII* gene regions for *Ceratocystis* isolates in the AAC were not available in GenBank, the ex-type cultures of relevant *Ceratocystis* species were sequenced to obtain the required datasets (Table 1). Sequences were aligned using mafft v. 7 (http://mafft.cbrc.jp/align-ment/server; Katoh *et al*., 2002), and then confirmed manually in mega v. 7.

For tree construction, maximum parsimony (MP) and maximum likelihood (ML) analyses were applied to each gene dataset as well as to a five-gene combined dataset. Before conducting combined analyses for sequences of the five gene regions, a partition homogeneity test (PHT) implemented in paup, was used to determine whether conflict existed between the datasets (Farris *et al*., 1995; Huelsenbeck *et al*., 1996). MP analyses were performed using paup v. 4.0b10* (Swofford, 2003). Uninformative characters were excluded and all informative characters were unordered and of equal weight, and gaps coded as a fifth character state. The most parsimonious trees (MPTs) were generated using a heuristic tree search criterion, including random stepwise addition of 1000 replicates and tree-bisection-reconstruction (TBR) branch-swapping. Statistical support for branch nodes in the MPTs was assessed with 1000 bootstrap replicates. Other parameters estimated for

MPTs included the tree length (TL), retention index (RI), consistency index (CI) and rescaled consistency indices (RC).

Maximum likelihood (ML) analyses were conducted for each dataset with PhyML v. 3.1 (Guindon & Gascuel, 2003). The most appropriate model for each dataset was obtained using the software package jModeltest v. 1.2.5 (Posada, 2008). Confidence levels for the nodes were determined using 1000 bootstrap replicates. Final consensus trees were viewed in mega v. 7 (Tamura *et al*., 2007). For both MP and ML analyses, *Ceratocystis albifundus* (CMW 4068) was used as the out-group taxon for the *BT1*, *TEF-1*α, *MS204*, *RPBII* and the combined datasets. For the ITS gene region, *Davidsoniella virescens* (CMW 11164) was used as the out-group.

Microsatellite amplification and genetic analyses

Allele scoring and genotyping

The genetic diversity of 99 isolates, including 31 isolates collected from *C. esculenta* corms in this study, six isolates of *Ceratocystis* sp. 'Y' (Li *et al*., 2017), 40 isolates of *C. cercfabiensis* (Liu *et al*., 2015), as well as 22 isolates for 10 other *Ceratocystis* species in the AAC (Table S1), was determined using 32 previously developed microsatellite markers (Barnes *et al*., 2001; Steimel *et al*., 2004; Fourie *et al*., 2016). Amplification reactions were performed in a total volume of 25 µL as described above, using the same conditions described by the authors that had developed the markers with slight modifications in annealing temperatures.

The microsatellite amplicons were analysed in three panels with GeneScan on an ABI 3500xl Autosequencer (Thermo Fisher Scientific). GeneScan Liz500(-250) size standard (Applied Biosystems) was used as the internal size standard. GeneScan data were analysed with GeneMapper v. 4.1 software (Applied Biosystems) to score fragment lengths as alleles. The combination of alleles for each isolate provided a multilocus genotype (MLG).

The MLGs of all 99 isolates in the AAC were compared to detect novel and shared genotypes as well as private alleles in the species. Isolates of the same species that shared identical MLGs were considered to be clones. A clone-corrected dataset was assembled in which each haplotype was represented once per species. This clone-corrected dataset was used for most of the analyses unless otherwise mentioned. popgene v. 1.31 (Yeh *et al*., 1999) was used to calculate the total number of alleles, the number of private alleles for each locus, and the allelic frequencies for each species.

UPGMA analyses

To assess relationships among the isolates collected from *C. esculenta* corms in this study as well as for the *Ceratocystis* species in the AAC, all the polymorphic microsatellite markers were used to determine their MLGs. The genetic distance between all the species in the AAC and the proportion of shared alleles were determined with the software populations v. 1.2.32 (Langella, 1999), using a Nei's minimum distance measure and a distance matrix. Subsequently, an unweighted pair group method with arithmetic mean (UPGMA), total

character difference tree was constructed in the same software to visualize the calculated distances, using 1000 bootstrap replications to ensure the results are statistically significant.

Morphological comparisons

Isolates collected from *C. esculenta* in this study were characterized based on structure morphology, culture morphology and optimal temperature for growth on 2% MEA. Sexual and asexual structures from selected 3-week-old cultures were mounted in 80% lactic acid on glass slides and examined using an Axioskop microscope (Carl Zeiss). Fifty measurements were made for each structure for the isolate chosen to represent the holotype and 10 measurements were taken for each structure of two additional isolates treated as paratypes. All measurements were computed and presented as (minimum–) mean minus SD – mean plus SD (–maximum). Colony morphology and colour (upper and reverse surfaces) were determined using the colour charts of Rayner (1970). To determine the optimal temperature for growth, three cultures (CMW 43272, CMW 43273, CMW 43281) were incubated at temperatures ranging from 5 to 35 °C at five-degree intervals, measurements were taken as described by Liu *et al*. (2015).

Pathogenicity tests

Pathogenicity on C. esculenta and E. japonica

To consider the pathogenicity of the *Ceratocystis* species from *C. esculenta*, and thus to fulfil Koch's postulates, inoculations were made on *C. esculenta* corms. In this experiment, four representative *Ceratocystis* isolates (CMW 43268, CMW 43273, CMW 43280, CMW 43281) obtained from different *C. esculenta* corms were used.

Isolates were grown on 2% MEA at 25 °C for 2 weeks. MEA plugs of 5 mm in diameter, covered with mycelium, were cut from the edges of the actively growing colonies. These plugs were used to inoculate 20 *C. esculenta* corms for each of the four test isolates and an equal number were inoculated with sterile MEA plugs to serve as negative controls. Wounds, approximately 2 mm deep, were made on the surfaces of the corms using a cork borer (5 mm diameter) and the MEA plugs were transferred, mycelium surface facing downwards, into the holes, which were then sealed with Parafilm. Inoculated corms were placed in sealed plastic boxes, the bases of which were lined with moist paper to retain humidity. These boxes were kept in a growth chamber and subjected to a constant temperature of 25 °C with natural day/night conditions for a period of 20 days.

The four *C. esculenta* isolates (CMW 43268, CMW 43273, CMW 43280, CMW 43281) were also inoculated onto the stems of *E. japonica* saplings, because they had ITS sequences identical to the *E. japonica* isolates considered by Li *et al*. (2014a). The *E. japonica* saplings used for inoculations were 1.5 years old, 60–80 cm in height and had diameters ranging from 1.0 to 1.2 cm. After acclimatization in a shade house for 2 weeks, 20 *E. japonica* saplings were inoculated with each of the four isolates. Wounds were made approximately 30 cm above the soil surface using a 5-mm-diameter cork borer to expose the cambium. MEA plugs covered with mycelium were placed into the wounds using the same method

employed for the *C. esculenta* corms. Twenty additional saplings were inoculated in the same way but with sterile MEA plugs to serve as negative controls.

Results were recorded after 3 weeks for *C. esculenta* and after 4 weeks for the *E. japonica* trial. This was done by measuring the lesion lengths (including the cork-borer wound) for each treatment. Reisolations were made from these lesions by cutting small pieces of corm/wood from the lesion edges and transferring these to 2% MEA and incubating the plates at 25 °C. Reisolations were made from four randomly selected corms and eight saplings for each isolate and from all the control inoculations. Results of all trials were analysed in excel (2013) using single factor analysis of variance (ANOVA) to test the effects of *Ceratocystis* isolate on lesion length. *F*-values with $P < 0.05$ were considered significantly different. The standard errors of means of lesion/wound length for each isolate and the controls were calculated.

Comparison of isolate aggressiveness and host susceptibility

In a second experiment, the host specificity was investigated of the isolates from *C. esculenta* and its close phylogenetic relative, *C. cercfabiensis*, recently described from *Eucalyptus* trees in China (Liu *et al*., 2015). Three isolates from *C. esculenta* (CMW 43272, CMW 43273, CMW 43281) and three *C. cercfabiensis* isolates (CMW 42515, CMW 42795, CMW 43029) obtained from *Eucalyptus* species (Liu *et al*., 2015) were used in a reciprocal inoculation onto both *C. esculenta* corms and *E. grandis* saplings. The six isolates were prepared as described above.

Twenty corms of *C. esculenta* and 20 *E. grandis* clone (CEPT-10) saplings (1-year-old, approximately 200 cm high, 1.0–1.2 cm diameter) were inoculated, using the method described above. Twenty additional corms and saplings were inoculated in the same way but with sterile MEA plugs to serve as negative controls.

In the second trial, results were read after 2 weeks for *C. esculenta* and 4 weeks for *E. grandis*, as described above.

Results

Fungal isolations

Abundant ascomata were found on the surfaces of the *C. esculenta* corms exhibiting black rot. In total, 31 isolates were obtained, of which 14 were from six diseased corms collected in the YunNan Province, and 17 were from eight diseased corms from the ShanDong Province. Based on morphological characteristics of the cultures and the ascomata produced on MEA, all the isolates were tentatively identified as species of *Ceratocystis*. These isolates grew relatively slowly on MEA and had a strong fruity (banana) odour. All isolates had brown to dark, globoid ascomata with long necks, without spines on their bases, and they produced hat-shaped, sheathed ascospores. Both bacilliform and barrel-shaped conidia were observed and cultures also produced dark aleurioconidia in chains.

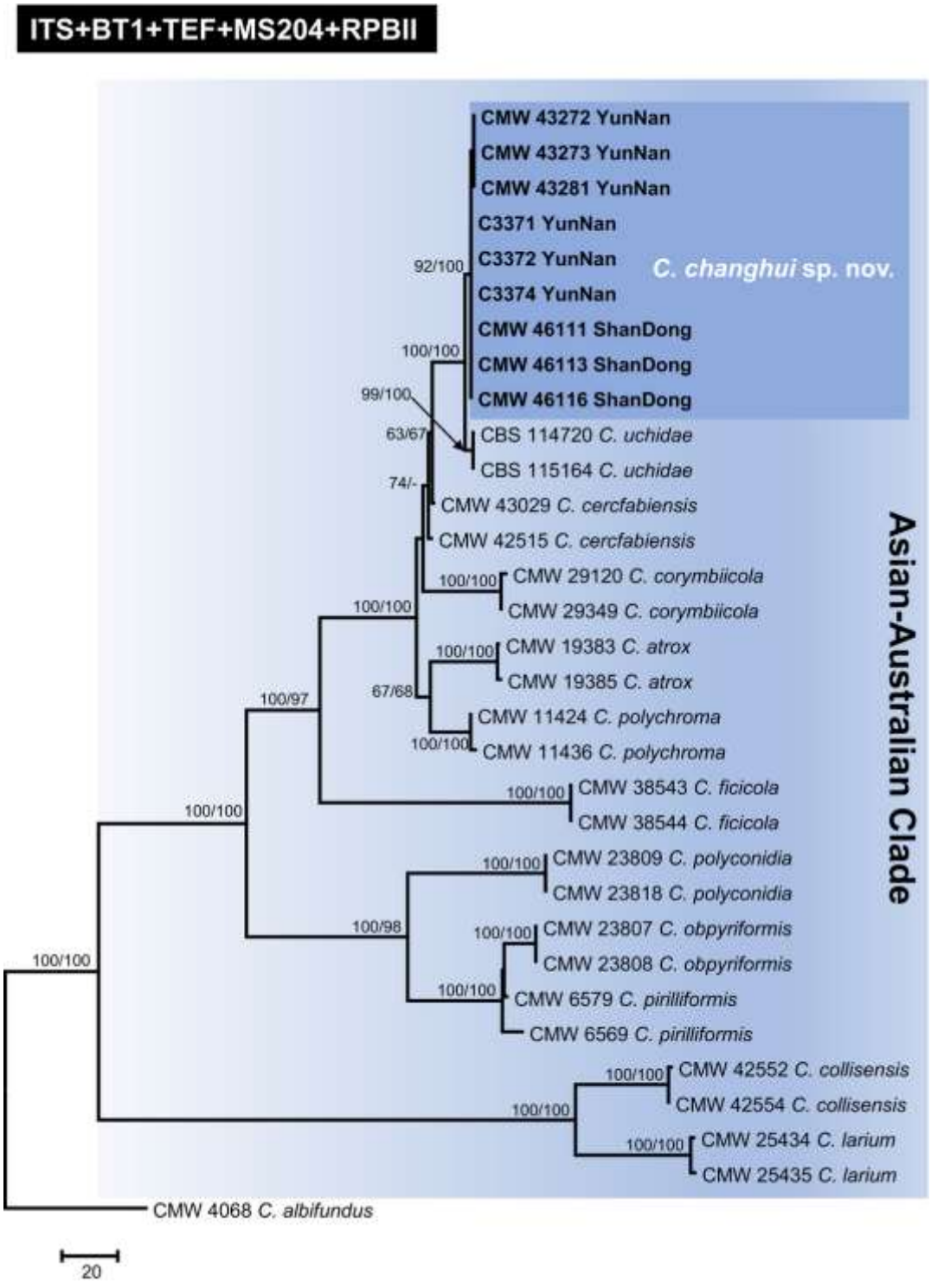

Figure 2. Phylogenetic trees based on maximum parsimony (MP) analysis of a combined dataset of ITS, *BT1*, *TEF-1*α, *MS204* and *RPBII* gene sequences for *Ceratocystis* species in the Asian-Australian clade. Isolates in bold and highlighted are the new species of *Ceratocystis changhui* described in this study. Bootstrap values >50% for MP and maximum likelihood (ML) are presented above branches as MP/ML, bootstrap values absent are not shown or marked with –. Scale bar indicates 20 changes.

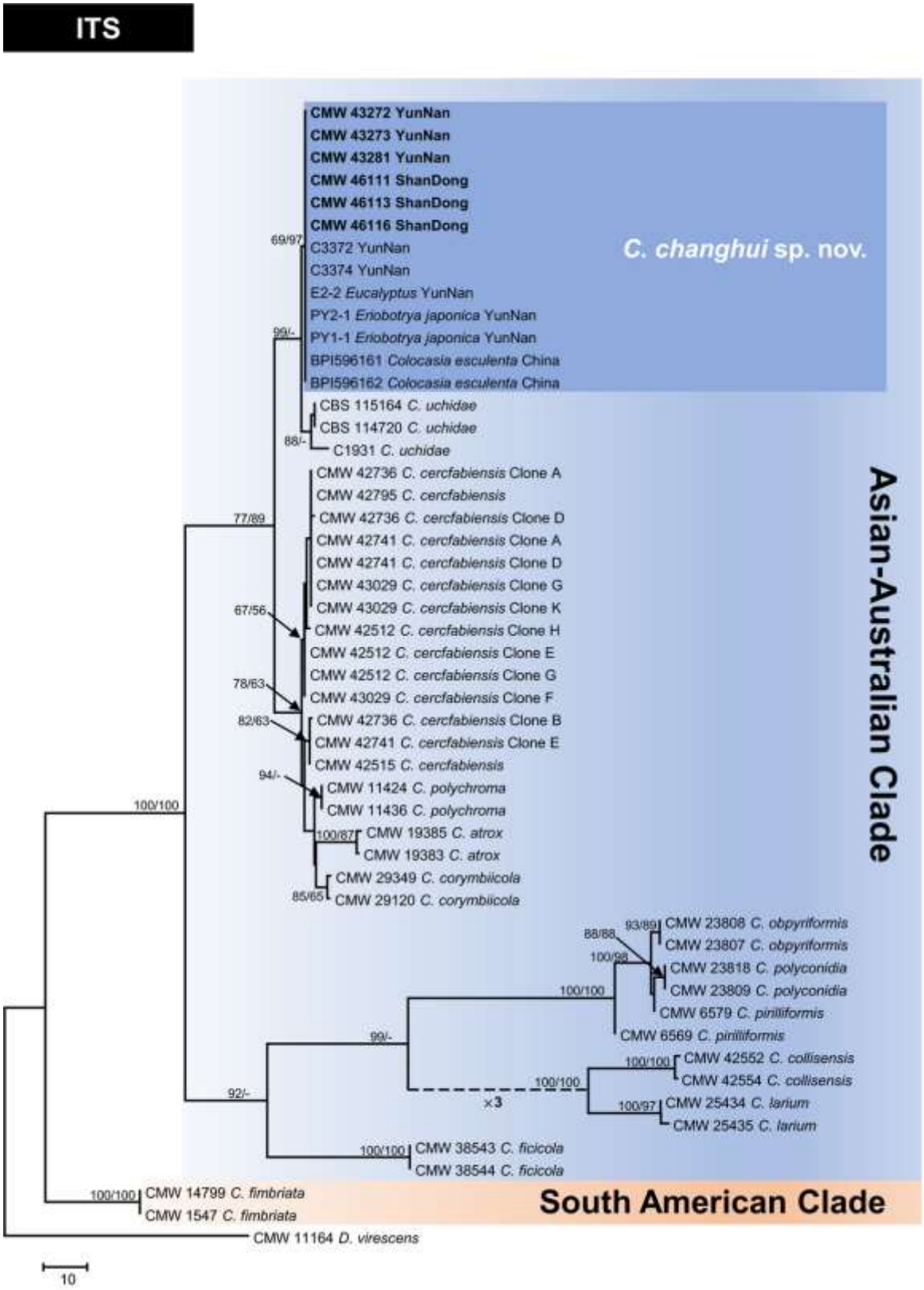

Figure 3. Phylogenetic trees based on maximum parsimony (MP) analysis of datasets of ITS sequences for *Ceratocystis* species in the Asian-Australian clade. Isolates in bold and highlighted are the new species of *Ceratocystis changhui* described in this study. Bootstrap values >50% for MP and maximum likelihood (ML) are presented above branches as MP/ML, bootstrap values absent are not shown or marked with –. The dotted line indicates that the length of the line has been shortened by a multiple of three. Scale bar indicates 10 changes.

Sequencing and multigene phylogenetic analyses

Sequencing of the ITS gene region was carried out for preliminary identification of the 31 isolates obtained from *C. esculenta* and the six isolates of *Ceratocystis* sp. 'Y' from *Eucalyptus* obtained from the study by Li *et al*. (2017). Subsequently, six *C. esculenta* isolates representing all of the areas sampled and three isolates of *Ceratocystis* sp. 'Y' were selected for further phylogenetic analyses (Table 1). These isolates were combined into datasets with the ex-type strains of the 11 AAC *Ceratocystis* species (*C. atrox*, *C. cercfabiensis*, *C. collisensis*, *C. corymbiicola*, *C. ficicola*, *C. larium*, *C. obpyriformis*, *C. piriliformis*, *C. polychroma*, *C. polyconidia*, *C. uchidae*; Table 1). PCRs resulted in amplicons of approximately 610, 610, 780, 970 and 1200 bp for the ITS, *BT1*, *TEF-1*α, *MS204* and *RPBII* loci, respectively. Partition homogeneity tests (PHT) with 1000 replicates for the five gene regions produced a value of $P = 0.001$, indicating some incongruence in the datasets for the five loci. Although the *P*-value was low, sequences of the multiple regions were combined for presentation purposes. The combined phylogeny and individual ITS phylogenies are presented in Figures 2 and 3, respectively. In addition, individual phylogenetic trees are presented in Figures S1, S2, S3 and S4.

All sequences obtained for the *Ceratocystis* isolates in this study were deposited in GenBank (Table 1), and a summary of the most important parameters applied in the phylogenetic analyses is presented in Table 2. The aligned sequences for the ITS (51 taxa, 711 characters), *BT1* (32 taxa, 553 characters), *TEF-1*α (32 taxa, 768 characters), *MS204* (32 taxa, 948 characters), *RPBII* (32 taxa, 1147 characters), and the combined (32 taxa, 4137 characters) datasets were deposited in TreeBASE (no. 21842).

The MP and ML analyses of the datasets provided trees with generally consistent topologies and phylogenetic relationships among taxa. The 11 *Ceratocystis* species in the AAC could be distinguished using a combination of five gene regions (Fig. 2). Among the five gene trees, the ITS tree gave the best resolution for separating all the species in the AAC (Fig. 3). However, some closely related species could not be separated by single gene trees (Figs S1, S2, S3 and S4). For example, the *MS204* gene tree could not distinguish between *C. cercfabiensis* and *C. uchidae*, *C. obpyriformis* and *C. pirilliformis* (Fig. S3). Likewise, the *RPBII* gene tree could not distinguish between *C. obpyriformis* and *C. pirilliformis* (Fig. S4).

Based on the MP and ML phylogenetic analyses, the isolates from *C. esculenta* in China formed a well-resolved lineage residing in the AAC in the ITS tree (Fig. 3), separated from all previously described *Ceratocystis* species (phylogenetic bootstrap value of MP/ML: 69%/97%). This lineage was supported by phylogenies based on the combined five gene trees (phylogenetic bootstrap value of MP/ML: 92%/100%, Fig. 2). However, in the separate *BT1*, *TEF-1*α, *MS204* and *RPBII* gene trees (Figs S1, S2, S3 and S4), the lineage was not distinct and could not be separated from *C. uchidae* or *C. cercfabiensis*. Similarly, not all gene regions could be used to distinguish all of the species in the AAC. Based on the phylogenetic analyses, the isolates from *C. esculenta* in China were considered as a putative new species.

Based on ITS sequence data, the *C. esculenta* isolates in this study were identical to isolates reported previously from *E. japonica* (E2-2) and *Eucalyptus* (PY1-1, PY2-1) by Li *et al*.

Table 2 Parameters used in all phylogenetic analyses in this study.

	ITS	*BT1*	*TEF-1α*	*MS204*	*RPBII*	Combined
No. of taxa	51	32	32	32	32	32
No. of bp[a]	711	553	768	948	1147	4137
PIC[b]	318	88	69	124	61	639
No. of trees	20	2	3	2	12	5
Tree length	604	112	108	152	81	991
CI[c]	0.813	0.920	0.731	0.901	0.852	0.809
RI[d]	0.930	0.967	0.888	0.958	0.945	0.921
HI[e]	0.187	0.080	0.269	0.099	0.148	0.191
Subst. model[f]	TPM1uf+G	HKY+I	TIM2+G	HKY+I	TrNef+I	TIM2+I+G
NST[g]	6	2	6	2	6	6
P-inv[h]	–	0.626	–	0.539	0.758	0.505
Gamma[i]	0.339	–	0.021	–	–	0.514

[a]Base pairs.
[b]Number of parsimony informative characters.
[c]Consistency index.
[d]Retention index.
[e]Homoplasy index.
[f]Best-fit substitution model.
[g]Number of substitution rate categories.
[h]Proportion of invariable sites.
[i]Distribution shape parameter.

(2014a,b), where they were referred to as *C. fimbriata s.l*. (Fig. 3). The ITS sequence was also identical to those from *C. esculenta* (BPI 596161, BPI 596162) and *Eucalyptus* (C3371–C3376) of the undescribed *Ceratocystis* sp. 'Y' (Fig. 3; Li *et al*., 2017). This suggests that the isolates from *C. esculenta* in the present study are the same as those previously studied (Thorpe *et al*., 2005; Li *et al*., 2014a,b, 2017).

Microsatellite amplification and genetic analyses

Allele scoring and genotyping

Of the 32 microsatellite markers tested, 23 were successfully amplified for all isolates and shown to be polymorphic for all but two isolates of one species, *C. corymbiicola*, in the AAC. For *C. corymbiicola*, 16 of the 23 markers produced multiple alleles that were difficult to score. As a result, this species was excluded from further analyses (Table S1). Alleles ranged from 2 to 10 at each locus, with a total of 139 alleles obtained from the 23 loci (Table S2). Forty-one unique MLGs were obtained when analysing the 23 polymorphic microsatellite loci across all isolates of the putative new species from *C. esculenta* in China and the other 10 species in the AAC.

Of the 41 different MLGs detected in the 97 isolates (Table S1), 20 were from *C. cercfabiensis* (40 isolates), 5 from the putative new species (37 isolates), 1 from *C. uchidae* (2 isolates), 1 from *C. atrox* (2 isolates), 2 from *C. pirilliformis* (2 isolates), 2 from *C. obpyriformis* (2 isolates), 2 from *C. larium* (2 isolates), 2 from *C. polychroma* (2 isolates), 3 from *C. collisensis* (4 isolates), 2 from *C. polyconidia* (2 isolates) and 1 from *C. ficicola* (2 isolates) (Fig. 4; Table S1). There were no shared MLGs among the putative new species and 10 other *Ceratocystis* species.

Of the 139 alleles obtained from the 23 loci, 79 alleles (56.8% of all 139 alleles) were private alleles (Table S2) and thus unique to a particular species. Among the 79 private alleles, there were 15 alleles (19.0%) from *C. ficicola*, 14 alleles (17.7%) from *C. polyconidia*, 9 alleles (11.4%) each from *C. collisensis* and *C. larium*, 7 alleles (8.9%) from *C. atrox*, 6 alleles (7.6%) from the new putative species, 5 alleles (6.3%) each from *C. cercfabiensis*, *C. uchidae* and *C. polychroma*, and 2 alleles (2.5%) each from *C. pirilliformis* and *C. obpyriformis* (Table S2). The high numbers of private alleles in each species reflected a high level of diversity and variation in *Ceratocystis* species residing in this clade.

UPGMA analyses

The genetic distance between isolates of the 10 *Ceratocystis* species in the AAC and the isolates of the putative new species from the present study (Fig. 4), provided results similar to those obtained from phylogenetic analyses. Here, all the isolates representing different species clustered together in the UPGMA (Fig. 4), providing additional support for species delimitation for the *Ceratocystis* species residing in the AAC. A total of 41 haplotypes were revealed in the UPGMA data where some species showed some low level of variation within species. A higher level of variation within species was clear, for example, within *C. pirilliformis* and *C. collisensis*. Although variation was observed in the isolates of *C. cercfabiensis*, the 20 MLGs from this species formed an independent clade. Even though

the *C. esculenta* isolates considered in this study were closely related to *C. cercfabiensis* and *C. uchidae*, they were clearly separated into a distinct clade in the UPGMA tree (Fig. 4).

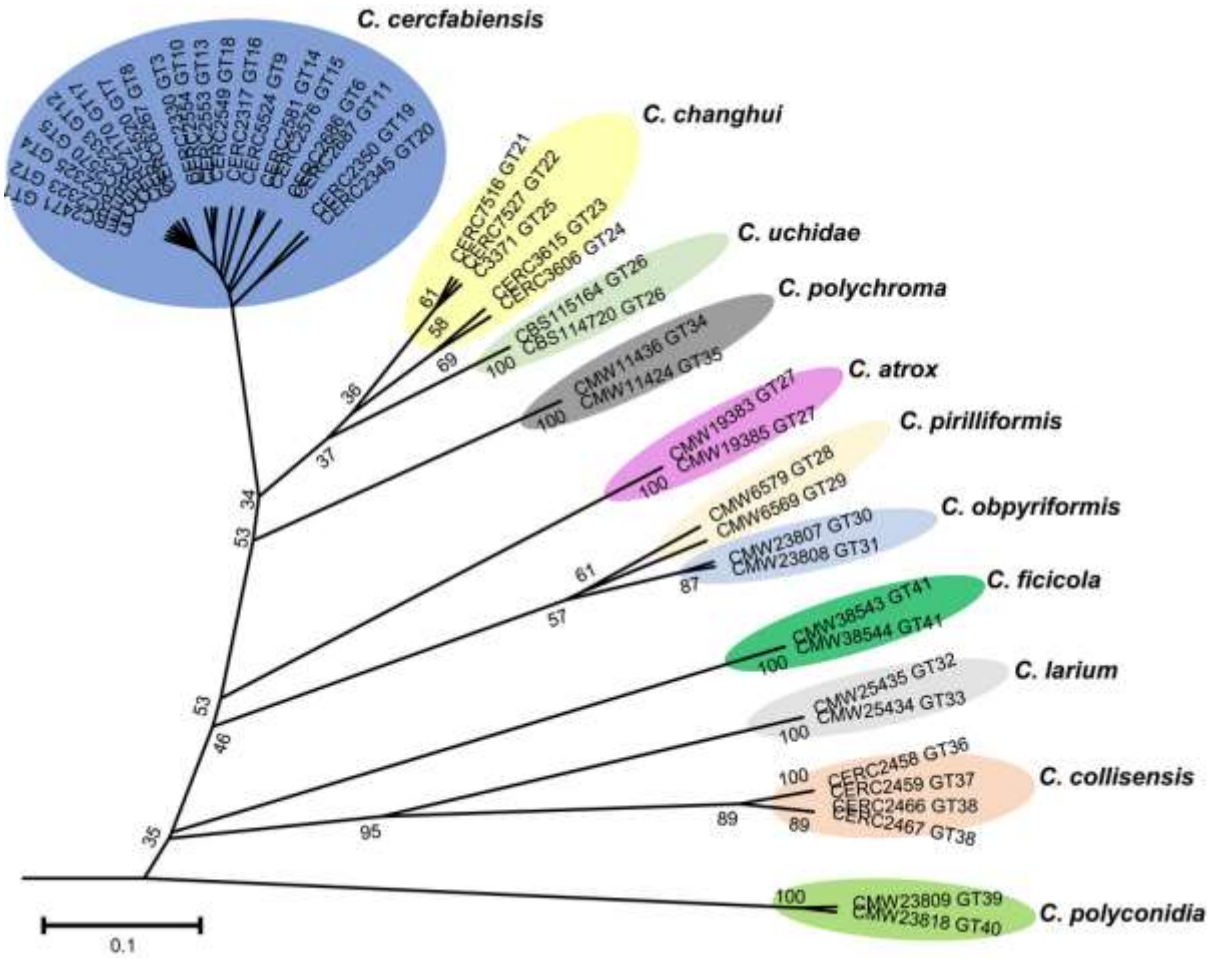

Figure 4. A UPGMA (unweighted pair group method, arithmetic mean) dendrogram of genotypes of *Ceratocystis* isolates in Asian-Australian clade based on alleles of 23 polymorphic microsatellite loci. Bootstrap values from 1000 replications are shown alongside the branches. Scale bar indicates genetic distance.

Morphological comparisons and taxonomy

Based on a phylogenetic analysis of five gene regions as well as an analysis of microsatellite data in a UPGMA tree, it was clear that the *Ceratocystis* species in the AAC could be clearly distinguished from each other. The isolates collected from *C. esculenta* in China that formed the basis of this study represent an undescribed taxon. It was most similar to *C. uchidae* and *C. cercfabiensis*, but could be distinguished from its closest relatives based on morphological differences including colour of the ascomatal bases, length of ostiolar hyphae, size of ascospores and size of cylindrical conidia (Table 3). A novel taxon is consequently described for these isolates as follows:

Table 3 Morphological comparison of Ceratocystis changhui with other phylogenetically closely related species.

	C. changhui	*C. uchidae*	*C. cercfabiensis*	*C. corymbiicola*	*C. polychroma*	*C. atrox*
Ascomata base	(139–)153.5–209(–261) × (132.5–)154–207.5(–257)	95–190 diam.	(100–)137–218.8(–302) × (79–)138–231(–286)	(159–)189–241(–290) × (160.5–)185.0–237.5(–272.5)	(208–)217–261(–269) diam.	(120–)140–180(–222) diam.
Ascomata base average	182.0 × 180.5	95.0–190.0 diam.	177.9 × 184.5	215.0 × 211.0	239.0 × 239.0	160.0 × 160.0
Ascomata neck	(453.5–)594–810(–896.5)	325–520	(473–)829–1400(–1756)	(603–)755–1009(–1097.5)	(837–)849–1071(–1187)	(277–)313–401(–451)
Ascomata neck average	702	422.5	1114.5	882	960	357
Ostiolar hyphae	(51–)58.5–105.5(–173)	40–75	(32–)48–70(–82)	(22.5–)42–58.5(–67.5)	(31–)33–43(–46)	(18–)20–26(–28)
Ostiolar hyphae average	82	57.5	59	50.3	38	23
Ascospores	(4.5–)5.0–6.0(–6.5) × (2.5–)3.0–3.5(–4.0)	4.0–6.0 × 2.0–3.5	(4 .1–)5.7–6.8(–7.5) × (2.5–)3.1–3.9(–4.6)	(4.5–)5.0–5.5(–6.0) × (2.5–)3.0–3.5(–4.0)	5–7 × 3–4	4–6 × 3–4
Ascospores average	5.5 × 3.5	5.0 × 2.75	6.3 × 3.5	5.3 × 3.3	6.0 × 3.5	5.0 × 3.5
Cylindrical conidia	(6.5–)10.5–16.5(–22.5) × (3.5–)4.5–5.5(–6.5)	10–25 × 2–4	(8.8–)16.2–25.6(–49.9) × (2.7–)3.4–4.6(–2.7)	(11.0–)15.0–21.5(–27.5) × (3.0–)3.5–4.5(–5.5)	(13–)16–24(–26) × 3–5	(9–)11–15(–17) × 3–5
Cylindrical conidia average	13.5 × 5.0	17.5 × 3.0	20.9 × 4.0	18.3 × 4.0	20.0 × 4.0	13.0 × 4.0
Barrel-shaped conidia	(3.5–)5.5–9.0(–10.5) × (3.5–)4.0–5.5(–6.0)	Not present	Not present	(7.5–)8.5–12.0(–14.5) × (3.5–)4.0–5.5(–6.5)	9–11 × 6–8	(7–)8–12(–14) × (5–)6–8(–9)
Barrel-shaped conidia average	7.0 × 4.5			10.3 × 4.8	10.0 × 7.0	10.0 × 7.0
Aleurioconidia	(8.5–)10.0–12.5(–14.0) × (6.0–)8.0–10.0(–11.5)	7.5–12.5 × 7.0–9.5	(9.9–)12.1–15.0(–16.7) × (7.0–)9.2–11.5(–13.0)	(8.5–)11.0–12.0(–16.5) × (6.5–)8.0–11.0(–16.5)	11–14 × 8–14	Not present
Aleurioconidia average	11.5 × 9.0	10.0 × 8.3	13.6 × 10.4	11.5 × 9.5	12.5 × 11.0	
Ascomata base colour	Brown, occasionally black	Black	Dark brown to black	Black	Dark brown to black	Dark brown to black

All measurements are in micrometres.

Ceratocystis changhui F.F. Liu, I. Barnes & S.F. Chen sp. nov. (Fig. 5)

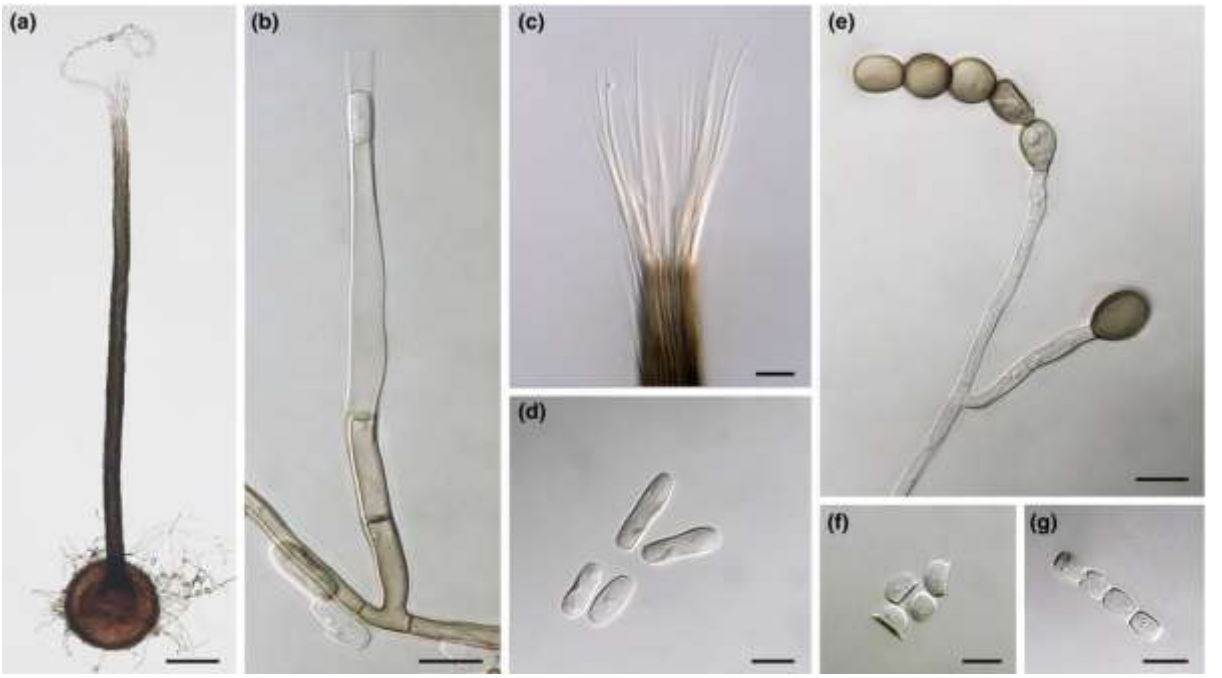

Figure 5. Morphological characteristics of *Ceratocystis changhui* sp. nov.: (a) ascomata with brown, globose to obpyriform base; (b) flask-shaped conidiophore; (c) divergent ostiolar hyphae; (d) various sizes of bacilliform conidia; (e) aleurioconidia in chains and solitary; (f) hat-shaped ascospores in side view and top view; (g) barrel-shaped conidia in a chain. Scale bars: a = 100 µm; b, d, e, g = 10 µm; f = 5 µm; c = 20 µm.

MycoBank MB815611

Etymology: the name is derived from the Chinese word for *Ceratocystis* (‘Changhui’).

Culture characteristics: Colonies on MEA olivaceous (21’’k), reverse olivaceous (21’’k). Mycelium immersed and superficial. *Hyphae* smooth, septate, without constriction at septa. Colony surfaces with scattered dark brown to black ascomata. Slow-growing, optimal temperature for growth 25 °C, no growth at 5, 10 or 35 °*C.* After 14 days, colonies at 15, 20, 25 and 30 °C reached 30.1, 38.8, 58.3 and 33.6 mm, respectively.

Sexual state: *Ascomatal bases* brown, occasionally black, globose to oval, semi-transparent, (139–)153.5–209(–261) µm long and (132.5–)154–207.5(–257) µm wide in diameter. Spines or ornamentations absent. *Ascomatal necks* dark brown to black, erect, slender, (453.5–)594–810(–896.5) µm long, (19.5–)24.5–35.5(–47) µm wide at apices and (28.5–)37–52.5(–63.5) µm wide at bases. *Ostiolar hyphae* present, hyaline, divergent, (51–)58.5–105.5(–173) µm long. *Asci* not observed. *Ascospores* hat-shaped, invested in sheaths, aseptate, (4.5–)5–6(–6.5) µm long and (2.5–)3–3.5(–4) µm wide with sheaths in side view. Ascospores accumulating in buff yellow (19 d) mucilaginous masses at the tips of ascomatal necks.

Asexual state: phialidic, with enteroblastic conidium ontogeny. *Conidiophores* flask-shaped producing bacilliform conidia, hyaline at apices, turning brown towards bases, multiseptate, lageniform, tubular, variable in size when terminal on hyphae, tapering at apices, (43.5–)60–95(–122) µm long, (3–)3.5–4.5(–6) µm wide at apices and (3.5–)4.5–6(–7.5) µm wide at

bases. *Bacilliform conidia* hyaline, aseptate, cylindrical, (6.5–)10.5–16.5(–22.5) µm long and (3.5–)4.5–5.5(–6.5) µm wide. *Barrel-shaped conidia* hyaline, aseptate, in chains, (3.5–)5.5–9(–10.5) µm long and (3.5–)4–5.5(–6) µm wide. *Aleurioconidia* ovoid, smooth, dark brown, embedded in agar, produced in chains or single, (8.5–)10–12.5(–14) × (6–)8–10(–11.5) µm in size.

Substrate: Black rot of *Colocasia esculenta* (taro) in China.

Distribution: YunNan and ShanDong Provinces, China.

Specimen examined: China, YunNan Province, KunMing Region, ChangShui Town, farm market. Isolated from lesions of black rot on *Colocasia esculenta*, August 2014, S.F. Chen. Dried specimens were deposited with the National Collection of Fungi (PREM), Pretoria, South Africa. HOLOTYPE PREM 61241, culture ex-type CMW 43281 = CERC 3615 = CBS 139797. GenBank accession numbers are KY643884, KY643919, KY643941, KY643962 and KY644015 for ITS, *BT1*, *TEF*, *MS204* and *RPBII* gene regions, respectively.

Additional specimens: China, YunNan Province, KunMing Region, ChangShui Town, farm market isolated from lesions of black rot on *Colocasia esculenta*, August 2014, S.F. Chen. Dried specimens were deposited with PREM. PARATYPE PREM 61242, culture CMW 43272 = CERC 3605 = CBS 139798. GenBank accession numbers are KY643886, KY643915, KY643937, KY643958 and KY644011 for ITS, *BT1*, *TEF*, *MS204* and *RPBII* gene regions, respectively. PARATYPE PREM 61243, culture CMW 43273 = CERC 3606 = CBS 139799. GenBank accession numbers are KY643889, KY643916, KY643938, KY643959 and KY644012 for ITS, *BT1*, *TEF*, *MS204* and *RPBII* gene regions, respectively.

Notes. *Ceratocystis changhui* is phylogenetically most closely related to *C. uchidae* (Li *et al*., 2017) and *C. cercfabiensis* (Liu *et al*., 2015), but can be distinguished from these two species by the colour of the ascomatal bases and the lengths of their necks, ostiolar hyphae and conidia (Table 3). When grown on 2% MEA at 25 °C, the ascomatal bases of *C. changhui* are brown and semitransparent in contrast to those of *C. uchidae* and *C. cercfabiensis* that are mostly black. Ascomatal necks of *C. changhui* (average 702 µm) are longer than those of *C. uchidae* (average 422.5 µm) and shorter than those of *C. cercfabiensis* (average 1115 µm). Ostiolar hyphae of *C. changhui* (average 82 µm) are longer than those of *C. uchidae* (average 57.5 µm) and *C. cercfabiensis* (average 59.0 µm). Bacilliform conidia of *C. changhui* (average 13.5 × 5.0 µm) are shorter than those of *C. uchidae* (average 17.5 × 3.0 µm) and *C. cercfabiensis* (average 20.9 × 4.0 µm). Barrel-shaped conidia are present in *C. changhui*, but absent in *C. uchidae* and *C. cercfabiensis*. Based on DNA sequence data, *C. changhui* differed from *C. uchidae* at five fixed nucleotide bases in the ITS, 1 bp in the *TEF* gene and 1 bp in the *RPBII* gene regions. There were 16 fixed nucleotide differences between *C. changhui* and *C. cercfabiensis* in ITS region and two in the *BT1* gene region.

Pathogenicity tests

Pathogenicity on C. esculenta and E. japonica

After 3 weeks, all four *C. changhui* isolates (CMW 43268, CMW 43273, CMW 43280, CMW 43281) caused black rot (lesions) on *C. esculenta* corms, and ascomata of a *Ceratocystis* were abundant on the rotten surfaces of the corms. Lesions did not form on the corms serving as negative controls (Fig. S5). The mean comparison tests showed that the lesions caused by the four *C. changhui* isolates were all significantly larger ($P < 0.05$) than the wounds associated with the controls (Fig. 6).

Only small lesions were produced on the stems of the *E. japonica* saplings inoculated with the four *C. changhui* isolates (CMW 43268, CMW 43273, CMW 43280, CMW 43281). The mean comparison tests showed that the lesions produced by isolates CMW 43268 and CMW 43281 were significantly longer than the wounds associated with controls, while the average lesion lengths associated with isolates CMW 43273 and CMW 43280 were not significantly different from the wound tissue found on the controls (Fig. 6).

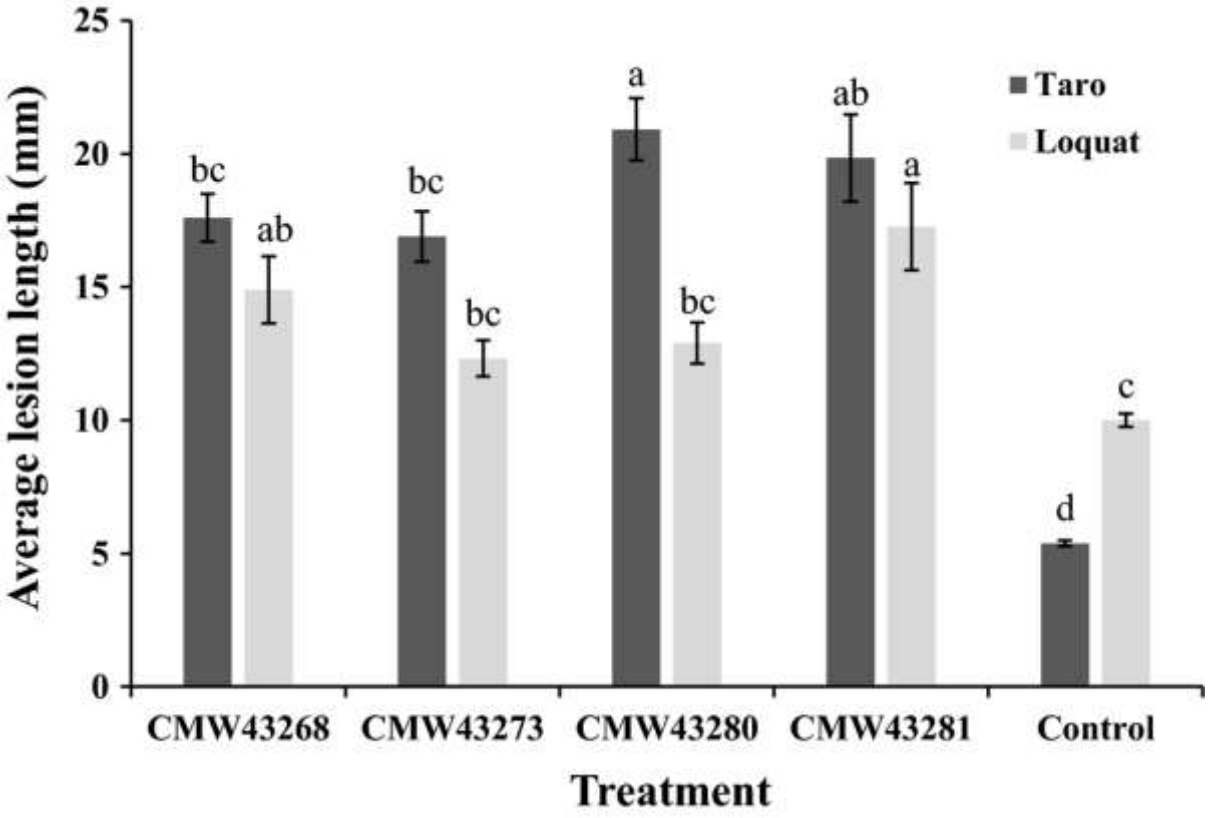

Figure 6. Bar graph showing the average lesion length (mm) resulting from inoculation trials with *Ceratocystis changhui* on corms of *Colocasia esculenta* (taro) and *Eriobotrya japonica* (loquat) saplings. Vertical bars represent standard error of means. Different letters above the bars indicate treatments that were significantly different ($P = 0.05$).

Comparison of isolate aggressiveness and host susceptibility

All three *C. changhui* isolates (CMW 43272, CMW 43273, CMW 43281) inoculated on *C. esculenta* corms caused black rot within 2 weeks. In contrast, only small lesions were produced by *C. cercfabiensis* (CMW 43029, CMW 42515, CMW 42795), and no rot was observed associated with the control inoculations. The mean comparison tests showed that the lesions caused by the *C. changhui* isolates were all significantly longer ($P < 0.05$) than those caused by *C. cercfabiensis* and the controls (Fig. 7). For the *Eucalyptus* inoculations, the three *C. cercfabiensis* isolates produced significantly longer lesions than those of the three *C. changhui* isolates ($P < 0.05$), while only small wound-associated discolouration was produced in the control inoculations (Fig. 7). The inoculated *Ceratocystis* spp. were reisolated from the lesions, but not from the controls.

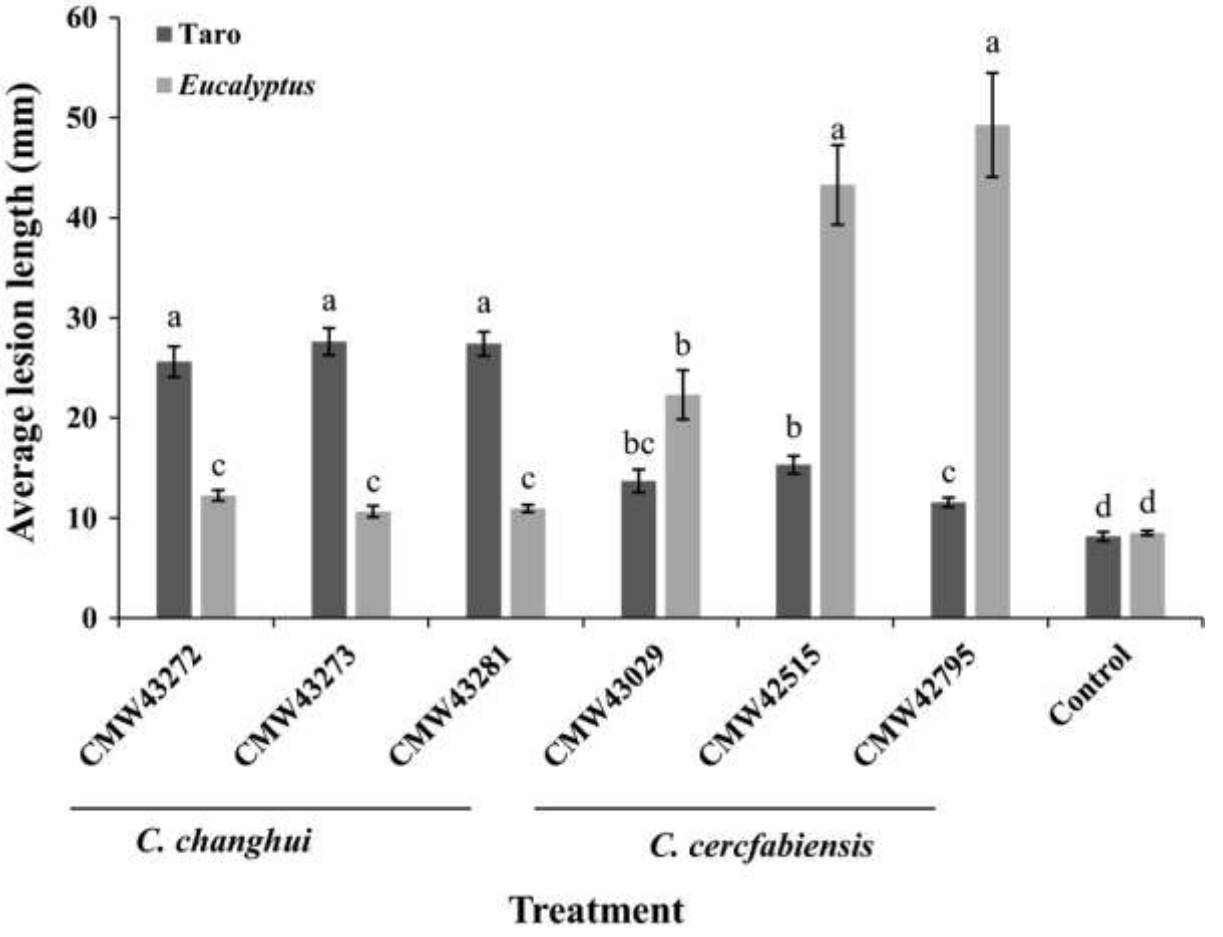

Figure 7. Bar graph showing the average lesion length (mm) resulting from inoculation trials with *Ceratocystis changhui* and *C. cercfabiensis* on corms of *Colocasia esculenta* (taro) and *Eucalyptus* saplings. Vertical bars represent standard error of means. Different letters above the bars indicate treatments that were significantly different ($P = 0.05$).

Discussion

This study led to the discovery of a new species of *Ceratocystis* that causes black rot symptoms on the corms of *C. esculenta* in the YunNan and ShanDong Provinces of China. This species, provided with the name *Ceratocystis changhui*, resides in the AAC of

Ceratocystis. The identity of *C. changhui* emerged from phylogenetic analyses for the ITS, *BT1*, *TEF-1*α, *MS204* and *RPBII* regions including a comparison with 11 previously described *Ceratocystis* species in the AAC. *Ceratocystis changhui* could also be distinguished from its closest relatives based on morphological characteristics. Furthermore, a UPGMA tree derived from microsatellite data provided additional support for the new species, where isolates clustered separately from 11 other species in the AAC. Pathogenicity tests showed that *C. changhui* can cause black rot disease on *C. esculenta* corms, but produced only small lesions on *E. grandis* and *E. japonica*.

Sequence comparisons for the ITS region showed that isolates of *C. changhui* described from *C. esculenta* in this study are identical to those of isolates obtained from *E. japonica* and *Eucalyptus* species by Li *et al*. (2014a,b). Based on phylogenetic analyses, the isolates previously reported by these authors and treated as *C. fimbriata s.l*. (LAC) more appropriately reside in the AAC. This is in contrast to *C. fimbriata s.s*. known to reside in the LAC (De Beer *et al*., 2014; Mbenoun *et al*., 2014; Fourie *et al*., 2015). Consequently, based on identical ITS sequences (100%), it is highly likely that the isolates from *E. japonica* and *Eucalyptus* sp. reported by Li *et al*. (2014a,b) also represent *C. changhui*, described here. However, this view should be tested with sequences for additional gene regions, which was not possible in the present study because appropriate isolates were not available. The ITS sequence of *C. changhui* was also identical to *Ceratocystis* sp. 'Y' reported by Li *et al*. (2017), including two isolates from *C. esculenta* imported to the USA from China in 1949 (Thorpe *et al*., 2005; Li *et al*., 2017) and six isolates from *Eucalyptus* species. The six *Eucalyptus* isolates were obtained and sequenced in the present study and, based on phylogenetic analyses for five gene regions, these isolates of *Ceratocystis* sp. 'Y' represent *C. changhui*.

Phylogenetic analyses of multiple gene regions are essential when seeking to identify species in *Ceratocystis* (De Beer *et al*., 2014; Fourie *et al*., 2015). The five gene regions selected for this purpose emerged from the study of Fourie *et al*. (2015), which showed that these genes can be collectively used to accurately delineate species in the AAC of *Ceratocystis*. Currently, 12 species of *Ceratocystis* are known in the AAC. Among the five gene regions, ITS was the most variable and informative region, clearly distinguishing between all of these species. The *BT1* and *TEF-1*α gene regions were also useful but with fewer variable sites. *BT1* could not distinguish between *C. changhui* and *C. uchidae*, and *TEF-1*α could not distinguish between *C. changhui* and *C. cercfabiensis*. *MS204* had the lowest number of variable sites and although seven species could be distinguished from each other, it was not possible to distinguish between *C. changhui*, *C. uchidae* and *C. cercfabiensis* with this marker. *RPBII* could not distinguish between *C. changhui* and *C. cercfabiensis*. *Ceratocystis obpyriformis* and *C. pirilliformis* could not be separated from each other using *MS204* or *RPBII*. Nevertheless, *C. changhui* could be clearly distinguished from its closest relatives when using a combination of sequences for the five gene regions.

UPGMA analyses of MLGs based on microsatellite markers gave additional support to distinguish *C. changhui* from all other species in the AAC. All isolates analysed in this study clustered in 11 different clades that represented the 11 described *Ceratocystis* species accommodated in the AAC. Within the clusters representing species, a high level of variation between isolates was observed. In addition, based on genetic distance, there was a close relationship between *C. changhui*, *C. cercfabiensis* and *C. uchida*e, which was similar to that

emerging from the phylogenetic analyses. Results also identified five different MLGs amongst the *C. changhui* isolates, which indicated that this species is not clonal in China. Results presented by Li *et al*. (2017) suggested that *C. cercfabiensis* could be an interspecific hybrid and that *C. uchidae* might be one of the hybrid parents, although data were not presented to support this view. UPGMA analyses in the present study showed high genetic diversity of *C. cercfabiensis*; the 20 MLGs of this species grouped in an independent clade and did not merge with other species in the AAC. These analyses, based on microsatellite markers, provide no evidence of hybrids between species and this avenue of research should clearly be pursued.

Ceratocystis changhui is closely related to *C. uchidae*, which was described from Hawaii and Fiji by Li *et al*. (2017). In the ITS sequences, *C. changhui* differed by five and 11 bp from *C. uchidae* isolates CBS 114720/CBS 115164 (Hawaii) and C1931 (Fiji), respectively (Li *et al*., 2017). Li *et al*. (2017) conducted interfertility tests between *C. uchidae* and their species 'Y', and showed that they were not interfertile. Because the present study has shown that species 'Y' is the same as *C. changhui*, this provides additional evidence, based on the biological species concept, for the unique nature of *C. changhui*. Furthermore, *C. changhui* can be distinguished from *C. uchidae* based on morphological differences, including the fact that the ascomatal bases of *C. changhui* are brown and semitransparent while those of *C. uchidae* are mostly black. Ascomata in *C. changhui* also have longer ascomatal necks and ostiolar hyphae, as well as shorter bacilliform conidia than those of *C. uchidae*.

Ceratocystis changhui can be distinguished from *C. cercfabiensis* based on various morphological characteristics. These include the colour of the ascomatal bases as well as the sizes of their ostiolar hyphae and conidia. These two species could also have been distinguished by their ascomatal neck lengths, according to the original description of *C. cercfabiensis*; however, the study of Li *et al*. (2017) expanded the neck length range for *C. cercfabiensis*, which now overlaps with those for *C. changhui*.

Ceratocystis changhui is an aggressive pathogen causing typical black rot symptoms on corms of *C. esculenta*. Inoculation tests also showed that isolates of this species are able to cause only small lesions or wound-associated discolouration on *E. japonica* and *E. grandis* stems. This is in contrast to the closely related *C. cercfabiensis* that is more pathogenic to *E. grandis*, but does not cause serious rot on *C. esculenta* corms. The results of the present study are somewhat in contrast to those of Li *et al*. (2014a,b); however, those authors used different techniques, making reasonable comparisons difficult. In the present investigation, tree stems of *E. grandis* and *E. japonica* were inoculated and *C. changhui* was shown to be non-pathogenic. Nevertheless, results of pathogenicity tests suggested host preferences for *C. changhui* and *C. cercfabiensis* and this is similar to those found for various other *Ceratocystis* species (Baker *et al*., 2003; Marin *et al*., 2003; Oliveira *et al*., 2015b).

Two species of *Ceratocystis* are now known from tuber crops in China. In the present study, *C. changhui* in the AAC was isolated from *C. esculenta* in two provinces more than 2000 km from each other. *Ceratocystis fimbriata s.s*. in the LAC was reported from *I. batatas* in northern China (Sy, 1956). Tuber crops, especially *C. esculenta* and *I. batatas*, are widely planted in China and studies aimed at extending knowledge of the genetic diversity and biology of *Ceratocystis* species on these plants would be valuable. They would also support

integrated strategies for the management of *Ceratocystis* diseases of tuber crops in China and other regions of the world.

Acknowledgements

The authors are grateful to the National Natural Science Foundation of China (NSFC; project numbers: 31622019 and 31400546), the International Science & Technology Cooperation Program of China (project number: 2012DFG31830), the Tree Protection and Cooperation Programme (TPCP) and the National Research Foundation (NRF), South Africa, for financial support. They also acknowledge Professor T. C. Harrington, Department of Plant Pathology and Microbiology, Iowa State University, who supplied the six cultures of *Ceratocystis* sp. 'Y'.

References

Al Adawi AO, Barnes I, Khan IA et al., 2013. Ceratocystis manginecans associated with a serious wilt disease of two native legume trees in Oman and Pakistan. Australasian Plant Pathology 42, 179–93.

Baker CJ, Harrington TC, Krauss U, Alfenas AC, 2003. Genetic variability and host specialization in the Latin American Clade of Ceratocystis fimbriata. Phytopathology 93, 1274–84.

Barnes I, Gaur A, Burgess T, Roux J, Wingfield BD, Wingfield MJ, 2001. Microsatellite markers reflect intraspecific relationships between isolates of the vascular wilt pathogen Ceratocystis fimbriata. Molecular Plant Pathology 2, 319–25.

Chair H, Traore RE, Duval MF et al., 2016. Genetic diversification and dispersal of taro (Colocasia esculenta (L.) Schott). PLoS ONE 11, e0157712.

Chen SF, van Wyk M, Roux J, Wingfield MJ, Xie YJ, Zhou XD, 2013. Taxonomy and pathogenicity of Ceratocystis species on Eucalyptus trees in South China, including C. chinaeucensis sp. nov. Fungal Diversity 58, 267–79.

De Beer ZW, Duong TA, Barnes I, Wingfield BD, Wingfield MJ, 2014. Redefining Ceratocystis and allied genera. Studies in Mycology 79, 187–219.

De Beer ZW, Marincowitz S, Duong TA, Wingfield MJ, 2017. Bretziella, a new genus to accommodate the oak wilt fungus, Ceratocystis fagacearum (Microascales, Ascomycota). MycoKeys 27, 1–19.

Duong TA, De Beer ZW, Wingfield BD, Wingfield MJ, 2012. Phylogeny and taxonomy of species in the Grosmannia serpens complex. Mycologia 104, 715–32.

Engelbrecht CJB, Harrington TC, 2005. Intersterility, morphology, and taxonomy of Ceratocystis fimbriata on sweet potato, cacao and sycamore. Mycologia 97, 57–69.

Farris JS, Kallersjo M, Kluge AG, Bult C, 1995. Testing significance of incongruence. Cladistics 10, 315–9.

Fourie A, Wingfield MJ, Wingfield BD, Barnes I, 2015. Molecular markers delimit cryptic species in Ceratocystis sensu stricto. Mycological Progress 14, 1–18.

Fourie A, Wingfield MJ, Wingfield BD, Thu PQ, Barnes I, 2016. A possible centre of diversity in South East Asia for the tree pathogen, Ceratocystis manginecans. Infection, Genetics and Evolution 41, 73–83.

Glass NL, Donaldson GC, 1995. Development of primer sets designed for use with the PCR to amplify conserved genes from filamentous Ascomycetes. Applied and Environmental Microbiology 61, 1323–30.

Guindon S, Gascuel O, 2003. A simple, fast, and accurate algorithm to estimate large phylogenies by maximum likelihood. Systematic Biology 52, 696–704.

Halsted BD, 1890. Some fungous disease of sweet potato. Agricultural College Experiment Station Bulletin 76, 1–32.

Harrington TC, 2000. Host specialization and speciation in the American wilt pathogen Ceratocystis fimbriata. Fitopatologia Brasileira 25S, 262–3.

Harrington TC, Thorpe DJ, Marinho VLA, Furtado EL, 2005. First report of black rot of Colocasia esculenta caused by Ceratocystis fimbriata in Brazil. Fitopatologia Brasileira 30, 88–9.

Harrington TC, Kazmi MR, Al Sadi AM, Ismail SI, 2014. Intraspecific and intragenomic variability of ITS rDNA sequences reveals taxonomic problems in Ceratocystis fimbriata sensu stricto. Mycologia 106, 224–42.

Harrington TC, Huang Q, Ferreira MA, Alfenas AC, 2015. Genetic analyses trace the Yunnan, China population of Ceratocystis fimbriata on pomegranate and taro to populations on Eucalyptus in Brazil. Plant Disease 99, 106–11.

Huang Q, Zhu YY, Chen HR et al., 2003. First report of pomegranate wilt caused by Ceratocystis fimbriata in Yunnan, China. Plant Disease 87, 1150.

Huang Q, Wang YY, Zhao YY et al., 2008. First report of taro black rot caused by Ceratocystis fimbriata in China. Plant Pathology 57, 780.

Huelsenbeck JP, Bull JJ, Cunningham CW, 1996. Combining data in phylogenetic analysis. Trends in Ecology & Evolution 11, 152–8.

Jacobs K, Bergdahl DR, Wingfield MJ et al., 2004. Leptographium wingfieldii introduced into North America and found associated with exotic Tomicus piniperda and native bark beetles. Mycological Research 108, 411–8.

Katoh K, Misawa K, Kuma K, Miyata T, 2002. mafft: a novel method for rapid multiple sequence alignment based on fast Fourier transform. Nucleic Acids Research 30, 3059–66.

Kile GA, 1993. Plant diseases caused by species of Ceratocystis sensu stricto and Chalara. In: Wingfield MJ, Seifert KA, Webber JFF, eds. Ceratocystis and Ophiostoma: Taxonomy, Ecology and Pathogenicity. St Paul, MN, USA: American Phytopathological Society Press, 73–183.

Langella O, 1999. populations 1.2.30. [http://www.bioinformatics.org/populations]. Accessed 2 October 2015.

Li J, Gao JM, Han YH, Sun YX, Huang Q, 2014a. First report of Ceratocystis fimbriata-caused wilt of Eriobotrya japonica in China. Plant Disease 98, 1270.

J, Zhang Y, Xu KC et al., 2014b. First report of wilt of Eucalyptus caused by Ceratocystis fimbriata in China. Plant Disease 98, 1744.

Li Q, Harrington TC, McNew D et al., 2016. Genetic bottlenecks for two populations of Ceratocystis fimbriata on sweet potato and pomegranate in China. Plant Disease 100, 2266–74.

Li Q, Harrington TC, McNew D, Li J, 2017. Ceratocystis uchidae sp. nov., a new species on Araceae in Hawaii and Fiji. Mycoscience 58, 398–412.

Liu FF, Mbenoun M, Barnes I et al., 2015. New Ceratocystis species from Eucalyptus and Cunninghamia in South China. Antonie van Leeuwenhoek 107, 1451–73.

Marin M, Castro B, Gaitan A, Preisig O, Wingfield BD, Wingfield MJ, 2003. Relationships of Ceratocystis fimbriata isolates from Colombian coffee-growing regions based on molecular data and pathogenicity. Journal of Phytopathology 151, 395–405.

Mbenoun M, Wingfield MJ, Aimé D., Boyogueno B, Wingfield BD, Roux J, 2014. Molecular phylogenetic analyses reveal three new Ceratocystis species and provide evidence for geographic differentiation of the genus in Africa. Mycological Progress 13, 219–40.

Möller EM, Bahnweg G, Sandermann H, Geiger HH, 1992. A simple and efficient protocol for isolation of high molecular weight DNA from filamentous fungi, fruit bodies, and infected plant tissues. Nucleic Acids Research 20, 6115.

Nel WJ, Duong TA, Wingfield BD, Wingfield MJ, De Beer ZW, 2017. A new genus and species for the globally important, multi-host root pathogen Thielaviopsis basicola. Plant Pathology. https://doi.org/10.1111/ppa.12803.

Oliveira LS, Harrington TC, Ferreira MA et al., 2015a. Species or genotypes? Reassessment of four recently described species of the Ceratocystis wilt pathogen, C. fimbriata, on Mangifera indica. Phytopathology 105, 1229–44.

Oliveira LS, Harrington TC, Freitas RG, McNew D, Alfenas AC, 2015b. Ceratocystis tiliae sp. nov., a wound pathogen on Tilia americana. Mycologia 107, 986–95.

Posada D, 2008. jModelTest: phylogenetic model averaging. Molecular Biology and Evolution 25, 1253–6.

Rayner RW, 1970. A Mycological Colour Chart. Kew, UK: Commonwealth Mycological Institute and British Mycological Society.

Roux J, Wingfield MJ, 2009. Ceratocystis species: emerging pathogens of non-native plantation Eucalyptus and Acacia species. Southern Forests 71, 115–20.

Schoch CL, Seifert KA, Huhndorf S et al., 2012. Nuclear ribosomal internal transcribed spacer (ITS) region as a universal DNA barcode marker for fungi. Proceedings of the National Academy of Sciences of the United States of America 109, 6241–6.

Shimizu M, 1939. Black rot of dasheen. Pusan Customs Plant Inspection Report 1. Japan.

Steimel J, Engelbrecht CJB, Harrington TC, 2004. Development and characterization of microsatellite markers for the fungus Ceratocystis fimbriata. Molecular Ecology Notes 4, 215–8.

Swofford DL, 2003. paup*. Phylogenetic Analysis Using Parsimony (*And Other Methods). Version 4. Sunderland, MA, USA: Sinauer Associates.

Sy CM, 1956. Studies on the control of black rot (Ophiostoma fimbriatum) of sweet potato. Acta Phytopathologica Sinica 2, 81–95.

Tamura K, Dudley J, Nei M, Kumar S, 2007. mega 4: molecular evolutionary genetics analysis (MEGA) software version 4.0. Molecular Biology and Evolution 24, 1596–9.

Thorpe DJ, Harrington TC, Uchida JY, 2005. Pathogenicity, internal transcribed spacer-rDNA variation, and human dispersal of Ceratocystis fimbriata on the family Araceae. Phytopathology 95, 316–23.

Uchida JY, Aragaki M, 1979. Ceratocystis blight of Syngonium podophyllum. Plant Disease Reporter 63, 1053–6.

Van Wyk M, Wingfield BD, Al-Adawi AO, Rossetto CJ, Ito MF, Wingfield MJ, 2011. Two new Ceratocystis species associated with mango disease in Brazil. Mycotaxon 117, 381–404.

White TJ, Bruns T, Lee S, Taylor J, 1990. Amplification and direct sequencing of fungal ribosomal RNA genes for phylogenetics. In: Innis MA, Gelfand DH, Sninsky JJ, White TJ, eds. PCR Protocols: A Guide to Methods and Applications. New York, NY, USA: Academic Press, 315–22.

Xu B, Zheng XH, Guo WX, Zhou XP, He P, 2011. First report of pomegranate wilt caused by Ceratocystis fimbriata in Sichuan Province. Plant Disease 95, 776.

Yeh FC, Yang RC, Boyle T, 1999. popgene. Version 1.31. Microsoft Windows-based Freeware for Population Genetic Analysis. Edmonton, Canada: University of Alberta.

Supplementary Material

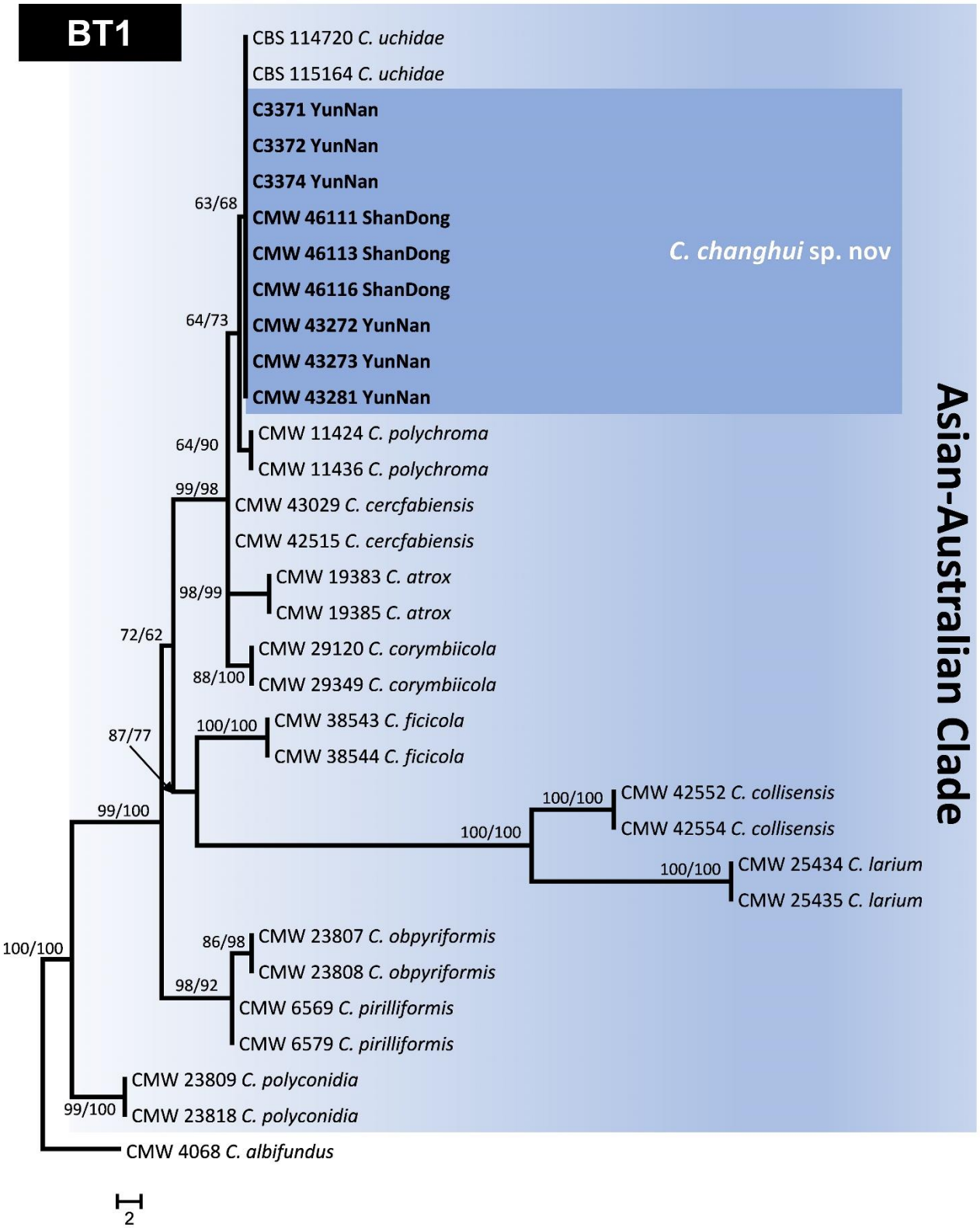

Figure S1. Phylogenetic trees based on maximum parsimony (MP) analysis of datasets of *BT1* gene sequences for *Ceratocystis* species in the Asian-Australian clade. Isolates in bold and highlighted are the new species of *Ceratocystis changhui* described in this study. Bootstrap values >50% for MP and maximum likelihood (ML) are presented above branches as MP/ML, bootstrap values absent are not shown or marked with –. The scale bar indicates 2 changes.

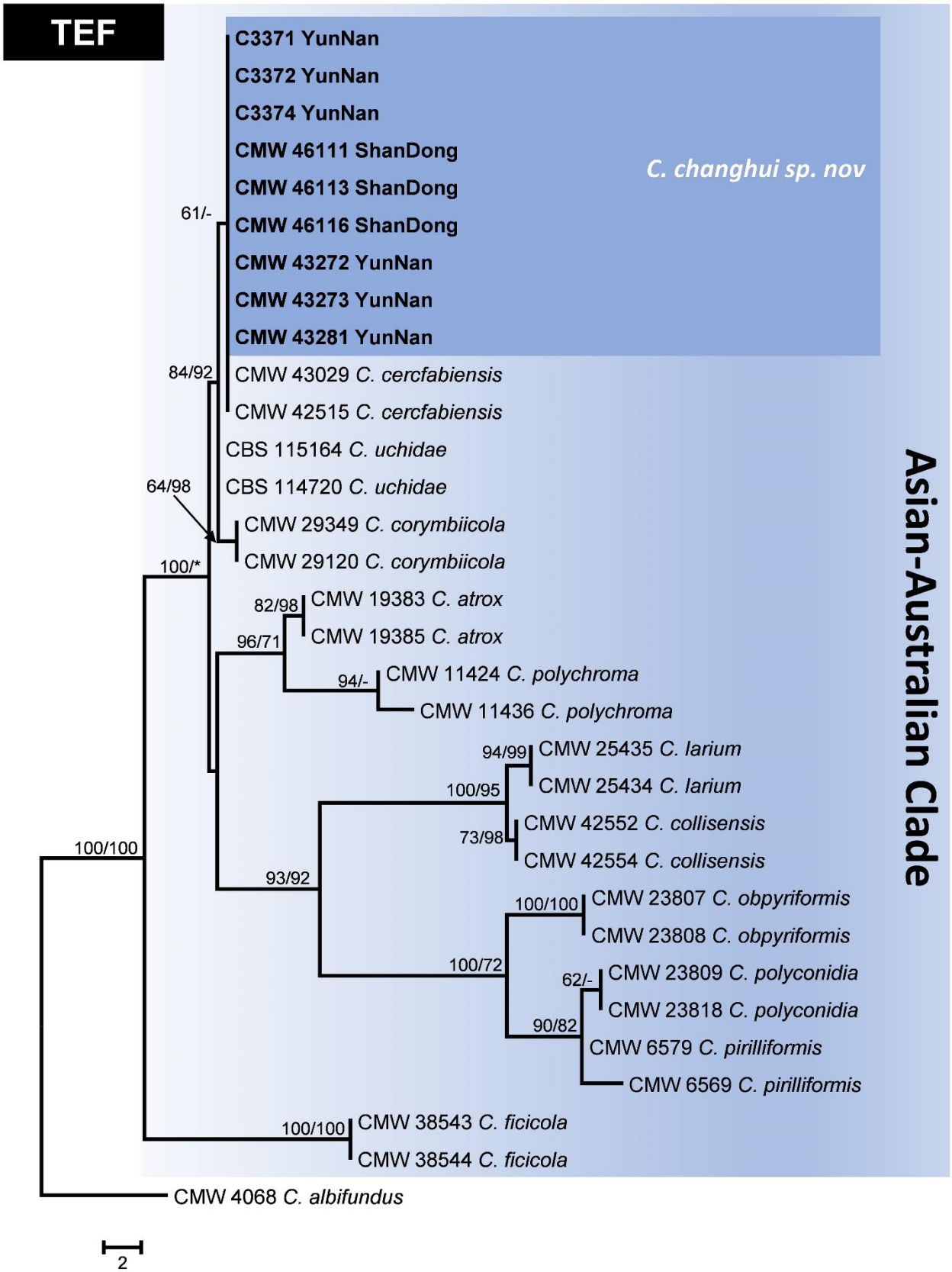

Figure S2. Phylogenetic trees based on maximum parsimony (MP) analysis of datasets of *TEF-1α* gene sequences for *Ceratocystis* species in the Asian-Australian clade. Isolates in bold and highlighted are the new species of *Ceratocystis changhui* described in this study. Bootstrap values >50% for MP and maximum likelihood (ML) are presented above branches as MP/ML, bootstrap values absent are not shown or marked with –. The scale bar indicates 2 changes.

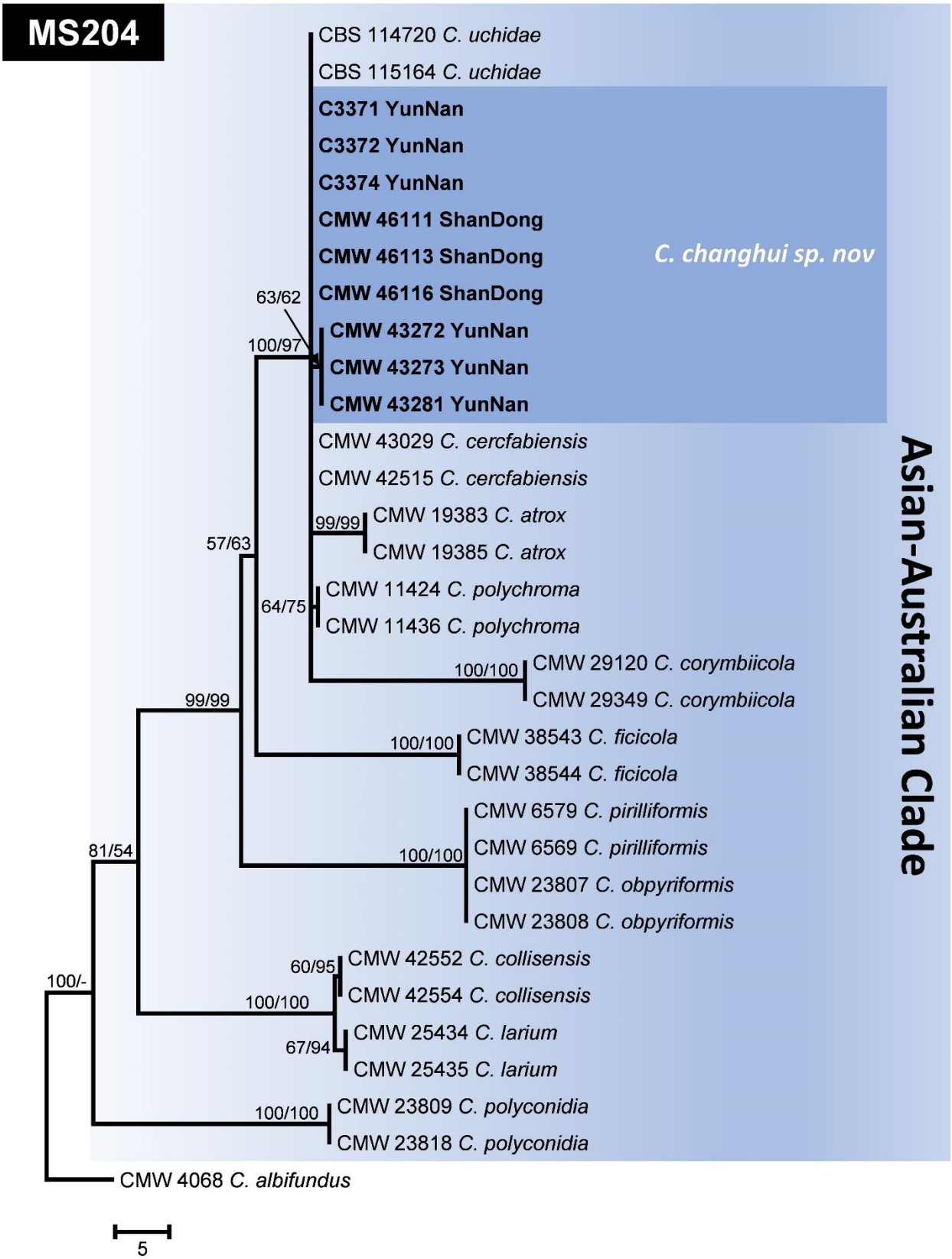

Figure S3. Phylogenetic trees based on maximum parsimony (MP) analysis of datasets of *MS204* gene sequences for *Ceratocystis* species in the Asian-Australian clade. Isolates in bold and highlighted are the new species of *Ceratocystis changhui* described in this study. Bootstrap values >50% for MP and maximum likelihood (ML) are presented above branches as MP/ML, bootstrap values absent are not shown or marked with –. The scale bar indicates 5 changes.

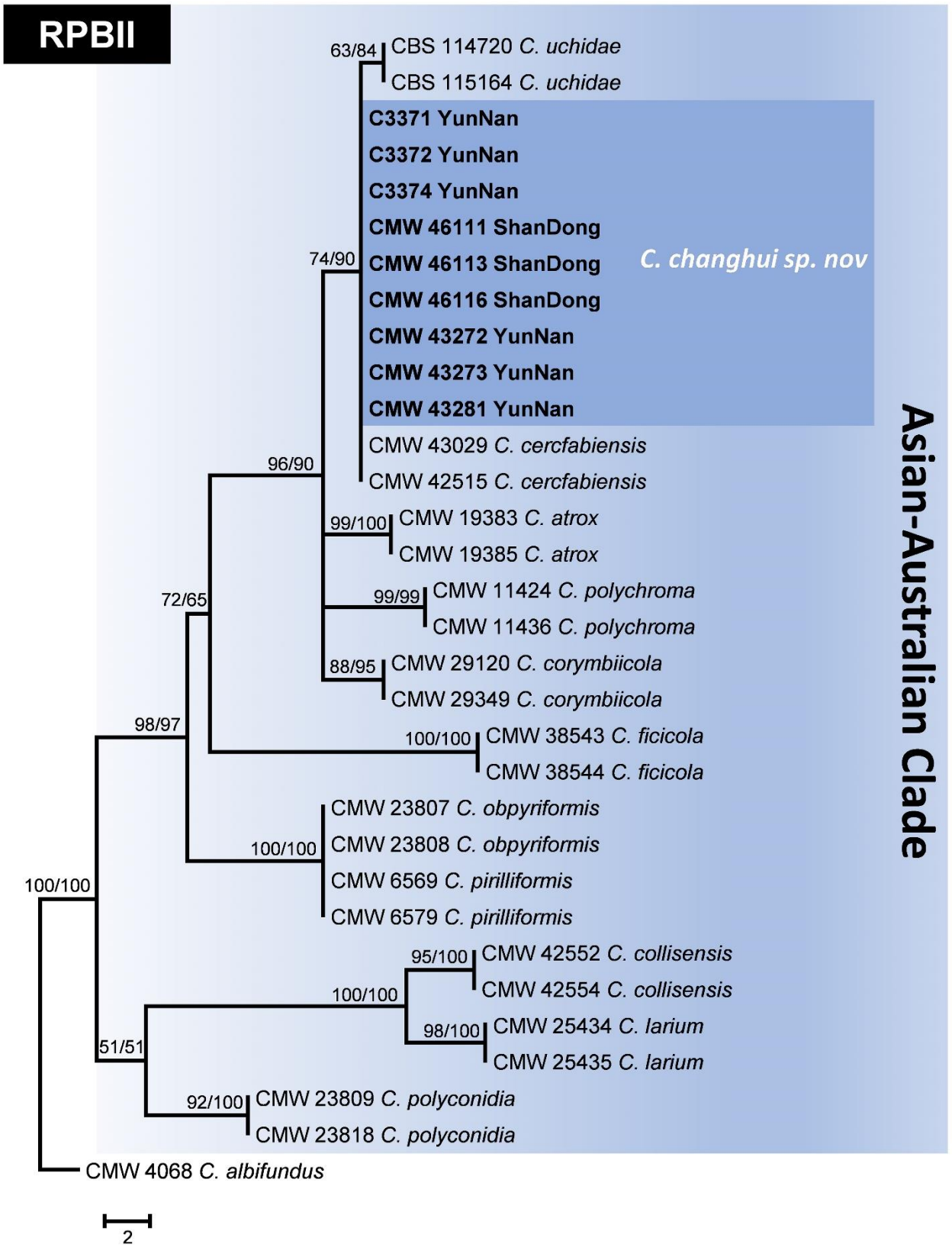

Figure S4. Phylogenetic trees based on maximum parsimony (MP) analysis of datasets of *RPBII* gene sequences for *Ceratocystis* species in the Asian-Australian clade. Isolates in bold and highlighted are the new species of *Ceratocystis changhui* described in this study. Bootstrap values >50% for MP and maximum likelihood (ML) are presented above branches as MP/ML, bootstrap values absent are not shown or marked with –. The scale bar indicates 2 changes.

Figure S5. Symptoms after inoculations of *Colocasia esculenta* corms with *Ceratocystis changhui* sp. nov. (Koch's postulates trials); (a) negative control showing wounds but the absence of lesions; (b) inoculation with *C. changhui* (CMW 43280), showing the lesions on the corm; (c) inoculation with *C. changhui* (CMW 43281), showing lesions on the longitudinal section of the corm. Bars: a, b = 20 mm.

Supplementary Table 1 List of *Ceratocystis* isolates included in the microsatellite study and the allele scoring results

Isolate	Species	Host	Location	MLG	AF2	AF3	AF4	AF5	AF6	AF7	AF9	AF11	CAA10	CAA38	GACA650	AG7/AG8	CF13/CF14	CF23/CF24	CAA9	AAG8	CAT1	AG1/AG2	CAA80	CAT9X	CAT3K	CAT1200	AAG9
CERC2471	*C. cercfabiensis*	*Eucalyptus*	FuJian	GT1	206	194	237	226	294	328	401	444	126	136	182	278	431	157	160	174	232	266	304	270	306	355	392
CERC2473	*C. cercfabiensis*	*Eucalyptus*	FuJian	GT1	206	194	237	226	294	328	401	444	126	136	182	278	431	157	160	174	232	266	304	270	306	355	392
CERC2475	*C. cercfabiensis*	*Eucalyptus*	FuJian	GT1	206	194	237	226	294	328	401	444	126	136	182	278	431	157	160	174	232	266	304	270	306	355	392
CERC2335	*C. cercfabiensis*	*Eucalyptus*	GuangXi	GT1	206	194	237	226	294	328	401	444	126	136	182	278	431	157	160	174	232	266	304	270	306	355	392
CERC2347	*C. cercfabiensis*	*Eucalyptus*	GuangXi	GT1	206	194	237	226	294	328	401	444	126	136	182	278	431	157	160	174	232	266	304	270	306	355	392
CERC2381	*C. cercfabiensis*	*Eucalyptus*	GuangXi	GT1	206	194	237	226	294	328	401	444	126	136	182	278	431	157	160	174	232	266	304	270	306	355	392
CERC2383	*C. cercfabiensis*	*Eucalyptus*	GuangXi	GT1	206	194	237	226	294	328	401	444	126	136	182	278	431	157	160	174	232	266	304	270	306	355	392
CERC2800	*C. cercfabiensis*	*Eucalyptus*	GuangXi	GT1	206	194	237	226	294	328	401	444	126	136	182	278	431	157	160	174	232	266	304	270	306	355	392
CERC2807	*C. cercfabiensis*	*Eucalyptus*	GuangXi	GT1	206	194	237	226	294	328	401	444	126	136	182	278	431	157	160	174	232	266	304	270	306	355	392
CERC2817	*C. cercfabiensis*	*Eucalyptus*	GuangXi	GT1	206	194	237	226	294	328	401	444	126	136	182	278	431	157	160	174	232	266	304	270	306	355	392
CERC2825	*C. cercfabiensis*	*Eucalyptus*	GuangXi	GT1	206	194	237	226	294	328	401	444	126	136	182	278	431	157	160	174	232	266	304	270	306	355	392
CERC2323	*C. cercfabiensis*	*Eucalyptus*	GuangXi	GT2	206	194	237	226	294	328	401	444	126	136	182	278	431	157	160	174	232	266	304	270	306	355	389
CERC2385	*C. cercfabiensis*	*Eucalyptus*	GuangXi	GT2	206	194	237	226	294	328	401	444	126	136	182	278	431	157	160	174	232	266	304	270	306	355	389
CERC2330	*C. cercfabiensis*	*Eucalyptus*	GuangXi	GT3	206	194	237	226	294	328	401	444	126	136	182	278	431	157	157	174	232	266	304	270	306	355	392
CERC2646	*C. cercfabiensis*	*Eucalyptus*	GuangXi	GT3	206	194	237	226	294	328	401	444	126	136	182	278	431	157	157	174	232	266	304	270	306	355	392
CERC2325	*C. cercfabiensis*	*Eucalyptus*	GuangXi	GT4	206	194	237	226	294	328	401	444	126	143	182	278	431	157	160	174	232	266	304	270	306	355	392
CERC2570	*C. cercfabiensis*	*Eucalyptus*	GuangDong	GT5	206	194	237	226	291	328	401	444	126	136	182	278	431	157	160	174	232	266	304	270	306	355	392
CERC2686	*C. cercfabiensis*	*Eucalyptus*	GuangDong	GT6	206	194	237	226	291	334	401	447	126	136	182	278	431	157	160	174	232	266	304	270	306	355	392
CERC5520	*C. cercfabiensis*	*Eucalyptus*	YunNan	GT7	206	194	237	226	288	328	401	444	126	136	182	278	431	157	160	174	232	266	304	270	306	355	392
CERC5526	*C. cercfabiensis*	*Eucalyptus*	YunNan	GT7	206	194	237	226	288	328	401	444	126	136	182	278	431	157	160	174	232	266	304	270	306	355	392
CERC5529	*C. cercfabiensis*	*Eucalyptus*	YunNan	GT7	206	194	237	226	288	328	401	444	126	136	182	278	431	157	160	174	232	266	304	270	306	355	392
CERC6276	*C. cercfabiensis*	*Eucalyptus*	YunNan	GT7	206	194	237	226	288	328	401	444	126	136	182	278	431	157	160	174	232	266	304	270	306	355	392
CERC6267	*C. cercfabiensis*	*Eucalyptus*	YunNan	GT8	206	194	237	226	288	328	401	444	126	136	182	278	431	157	160	174	232	266	304	270	M[2]	355	392
CERC5524	*C. cercfabiensis*	*Eucalyptus*	YunNan	GT9	206	194	237	226	288	328	401	444	M	136	182	278	431	157	160	174	232	266	304	270	M	355	397
CERC2554	*C. cercfabiensis*	*Eucalyptus*	GuangDong	GT10	206	194	237	226	N[1]	328	401	444	126	136	182	278	431	157	157	174	232	266	304	270	306	355	392
CERC2687	*C. cercfabiensis*	*Eucalyptus*	GuangDong	GT11	206	194	237	226	N	334	N	447	126	136	182	278	431	157	160	174	232	266	304	270	306	355	392
CERC2333	*C. cercfabiensis*	*Eucalyptus*	GuangXi	GT12	206	194	240	226	294	328	401	444	126	136	182	278	431	157	160	174	232	266	304	270	306	355	392
CERC2358	*C. cercfabiensis*	*Eucalyptus*	GuangXi	GT12	206	194	240	226	294	328	401	444	126	136	182	278	431	157	160	174	232	266	304	270	306	355	392
CERC2368	*C. cercfabiensis*	*Eucalyptus*	GuangXi	GT12	206	194	240	226	294	328	401	444	126	136	182	278	431	157	160	174	232	266	304	270	306	355	392
CERC2553	*C. cercfabiensis*	*Eucalyptus*	GuangDong	GT13	206	194	240	226	294	328	401	444	126	136	182	278	431	157	157	174	232	266	304	270	306	355	392
CERC2581	*C. cercfabiensis*	*Eucalyptus*	GuangDong	GT14	206	194	240	226	294	328	401	444	129	136	182	278	431	157	160	174	232	266	304	270	306	355	392
CERC2586	*C. cercfabiensis*	*Eucalyptus*	GuangDong	GT14	206	194	240	226	294	328	401	444	129	136	182	278	431	157	160	174	232	266	304	270	306	355	392
CERC2576	*C. cercfabiensis*	*Eucalyptus*	GuangDong	GT15	206	194	240	226	294	328	401	444	129	136	182	278	431	157	160	174	232	266	304	270	306	355	384
CERC2317	*C. cercfabiensis*	*Eucalyptus*	GuangXi	GT16	206	194	240	226	291	328	401	444	126	136	182	278	431	157	160	174	232	266	304	270	306	355	392
CERC2552	*C. cercfabiensis*	*Eucalyptus*	GuangDong	GT17	203	194	237	226	294	328	401	444	126	136	182	278	431	157	160	174	232	266	304	270	306	355	392
CERC2170	*C. cercfabiensis*	*Eucalyptus*	HaiNan	GT17	203	194	237	226	294	328	401	444	126	136	182	278	431	157	160	174	232	266	304	270	306	355	392
CERC2177	*C. cercfabiensis*	*Eucalyptus*	HaiNan	GT17	203	194	237	226	294	328	401	444	126	136	182	278	431	157	160	174	232	266	304	270	306	355	392

CERC2549	*C. cercfabiensis*	*Eucalyptus*	GuangDong	GT18	203	194	237	226	294	328	401	444	126	136	182	278	431	157	157	174	232	266	304	270	306	355	392
CERC2350	*C. cercfabiensis*	*Eucalyptus*	GuangXi	GT19	203	194	240	226	294	328	401	444	126	136	182	278	431	157	160	171	232	266	304	270	306	355	392
CERC2345	*C. cercfabiensis*	*Eucalyptus*	GuangXi	GT20	203	194	240	226	294	328	401	444	126	136	182	278	431	157	157	174	232	266	304	270	306	355	392
CERC7516	*C. changhui*	*Colocasia esculenta*	ShanDong	GT21	223	194	243	226	270	328	401	444	126	136	182	278	431	157	147	171	232	266	292	267	306	355	392
CERC7519	*C. changhui*	*Colocasia esculenta*	ShanDong	GT21	223	194	243	226	270	328	401	444	126	136	182	278	431	157	147	171	232	266	292	267	306	355	392
CERC7520	*C. changhui*	*Colocasia esculenta*	ShanDong	GT21	223	194	243	226	270	328	401	444	126	136	182	278	431	157	147	171	232	266	292	267	306	355	392
CERC7524	*C. changhui*	*Colocasia esculenta*	ShanDong	GT21	223	194	243	226	270	328	401	444	126	136	182	278	431	157	147	171	232	266	292	267	306	355	392
CERC7529	*C. changhui*	*Colocasia esculenta*	ShanDong	GT21	223	194	243	226	270	328	401	444	126	136	182	278	431	157	147	171	232	266	292	267	306	355	392
CERC7531	*C. changhui*	*Colocasia esculenta*	ShanDong	GT21	223	194	243	226	270	328	401	444	126	136	182	278	431	157	147	171	232	266	292	267	306	355	392
CERC7532	*C. changhui*	*Colocasia esculenta*	ShanDong	GT21	223	194	243	226	270	328	401	444	126	136	182	278	431	157	147	171	232	266	292	267	306	355	392
CERC7533	*C. changhui*	*Colocasia esculenta*	ShanDong	GT21	223	194	243	226	270	328	401	444	126	136	182	278	431	157	147	171	232	266	292	267	306	355	392
CERC7534	*C. changhui*	*Colocasia esculenta*	ShanDong	GT21	223	194	243	226	270	328	401	444	126	136	182	278	431	157	147	171	232	266	292	267	306	355	392
CERC7536	*C. changhui*	*Colocasia esculenta*	ShanDong	GT21	223	194	243	226	270	328	401	444	126	136	182	278	431	157	147	171	232	266	292	267	306	355	392
CERC7538	*C. changhui*	*Colocasia esculenta*	ShanDong	GT21	223	194	243	226	270	328	401	444	126	136	182	278	431	157	147	171	232	266	292	267	306	355	392
CERC7541	*C. changhui*	*Colocasia esculenta*	ShanDong	GT21	223	194	243	226	270	328	401	444	126	136	182	278	431	157	147	171	232	266	292	267	306	355	392
CERC7542	*C. changhui*	*Colocasia esculenta*	ShanDong	GT21	223	194	243	226	270	328	401	444	126	136	182	278	431	157	147	171	232	266	292	267	306	355	392
CERC7543	*C. changhui*	*Colocasia esculenta*	ShanDong	GT21	223	194	243	226	270	328	401	444	126	136	182	278	431	157	147	171	232	266	292	267	306	355	392
CERC7544	*C. changhui*	*Colocasia esculenta*	ShanDong	GT21	223	194	243	226	270	328	401	444	126	136	182	278	431	157	147	171	232	266	292	267	306	355	392
CERC7527	*C. changhui*	*Colocasia esculenta*	ShanDong	GT22	223	194	243	226	270	328	401	444	126	136	182	278	431	157	147	171	232	266	292	267	M	355	397
CERC7530	*C. changhui*	*Colocasia esculenta*	ShanDong	GT22	223	194	243	226	270	328	401	444	126	136	182	278	431	157	147	171	232	266	292	267	M	355	397
CERC3601	*C. changhui*	*Colocasia esculenta*	YunNan	GT23	220	194	237	226	270	328	401	444	126	143	182	278	431	157	147	171	232	266	304	267	306	355	392
CERC3602	*C. changhui*	*Colocasia esculenta*	YunNan	GT23	220	194	237	226	270	328	401	444	126	143	182	278	431	157	147	171	232	266	304	267	306	355	392
CERC3604	*C. changhui*	*Colocasia esculenta*	YunNan	GT23	220	194	237	226	270	328	401	444	126	143	182	278	431	157	147	171	232	266	304	267	306	355	392
CERC3605	*C. changhui*	*Colocasia esculenta*	YunNan	GT23	220	194	237	226	270	328	401	444	126	143	182	278	431	157	147	171	232	266	304	267	306	355	392
CERC3607	*C. changhui*	*Colocasia esculenta*	YunNan	GT23	220	194	237	226	270	328	401	444	126	143	182	278	431	157	147	171	232	266	304	267	306	355	392
CERC3608	*C. changhui*	*Colocasia esculenta*	YunNan	GT23	220	194	237	226	270	328	401	444	126	143	182	278	431	157	147	171	232	266	304	267	306	355	392
CERC3609	*C. changhui*	*Colocasia esculenta*	YunNan	GT23	220	194	237	226	270	328	401	444	126	143	182	278	431	157	147	171	232	266	304	267	306	355	392
CERC3610	*C. changhui*	*Colocasia esculenta*	YunNan	GT23	220	194	237	226	270	328	401	444	126	143	182	278	431	157	147	171	232	266	304	267	306	355	392
CERC3611	*C. changhui*	*Colocasia esculenta*	YunNan	GT23	220	194	237	226	270	328	401	444	126	143	182	278	431	157	147	171	232	266	304	267	306	355	392

CERC3612	*C. changhui*	*Colocasia esculenta*	YunNan	GT23	220	194	237	226	270	328	401	444	126	143	182	278	431	157	147	171	232	266	304	267	306	355	392
CERC3614	*C. changhui*	*Colocasia esculenta*	YunNan	GT23	220	194	237	226	270	328	401	444	126	143	182	278	431	157	147	171	232	266	304	267	306	355	392
CERC3615	*C. changhui*	*Colocasia esculenta*	YunNan	GT23	220	194	237	226	270	328	401	444	126	143	182	278	431	157	147	171	232	266	304	267	306	355	392
CERC3616	*C. changhui*	*Colocasia esculenta*	YunNan	GT23	220	194	237	226	270	328	401	444	126	143	182	278	431	157	147	171	232	266	304	267	306	355	392
CERC3606	*C. changhui*	*Colocasia esculenta*	YunNan	GT24	220	194	237	226	270	328	401	444	126	143	182	278	431	157	147	171	232	266	304	267	322	355	397
C3371	*Ceratocystis* sp. Y[3]	*Eucalyptus*	YunNan	GT25	232	194	243	226	270	328	401	444	126	136	182	M	431	157	147	171	232	266	292	267	306	355	392
C3372	*Ceeratocystis* sp. Y[3]	*Eucalyptus*	YunNan	GT25	232	194	243	226	270	328	401	444	126	136	182	M	431	157	147	171	232	266	292	267	306	355	392
C3373	*Ceratocystis* sp. Y[3]	*Eucalyptus*	YunNan	GT25	232	194	243	226	270	328	401	444	126	136	182	M	431	157	147	171	232	266	292	267	306	355	392
C3374	*Ceratocystis* sp. Y[3]	*Eucalyptus*	YunNan	GT25	232	194	243	226	270	328	401	444	126	136	182	M	431	157	147	171	232	266	292	267	306	355	392
C3375	*Ceratocystis* sp. Y[3]	*Eucalyptus*	YunNan	GT25	232	194	243	226	270	328	401	444	126	136	182	M	431	157	147	171	232	266	292	267	306	355	392
C3376	*Ceratocystis* sp. Y[3]	*Eucalyptus*	YunNan	GT25	232	194	243	226	270	328	401	444	126	136	182	M	431	157	147	171	232	266	292	267	306	355	392
CBS 115164	*C. uchidae*	*Colocasia esculenta*	Hawaii	GT26	219	194	249	226	270	329	401	444	126	139	182	278	446	157	147	171	232	266	284	267	306	355	392
CBS 114720	*C. uchidae*	*Colocasia esculenta*	Hawaii	GT26	219	194	249	226	270	329	401	444	126	139	182	278	446	157	147	171	232	266	284	267	306	355	392
CMW19383	*C. atrox*	*Eucalyptus grandis*	Australia	GT27	192	194	231	226	270	319	401	452	129	124	191	280	407	157	M	177	225	266	280	270	306	355	386
CMW19385	*C. atrox*	*Eucalyptus grandis*	Australia	GT27	192	194	231	226	270	319	401	452	129	124	191	280	407	157	M	177	225	266	280	270	306	355	386
CMW6579	*C. pirilliformis*	*Eucalyptus nitens*	Australia	GT28	192	194	234	230	270	340	399	450	126	93	177	278	382	157	140	159	219	266	304	267	306	357	384
CMW6569	*C. pirilliformis*	*Eucalyptus nitens*	Australia	GT29	206	194	231	230	270	340	399	450	129	93	177	278	382	157	140	183	219	266	304	267	306	357	384
CMW23807	*C. obpyriformis*	*Acacia mearnsii*	South Africa	GT30	192	194	228	230	252	340	399	452	126	93	177	278	382	157	140	177	219	266	304	270	306	357	384
CMW23808	*C. obpyriformis*	*Acacia mearnsii*	South Africa	GT31	192	194	228	230	252	340	399	450	126	93	177	278	382	157	140	177	219	266	304	270	306	357	384
CMW25435	*C. larium*	*Styrax benzoin*	Indonesia	GT32	203	194	218	234	270	310	422	476	135	130	177	278	431	160	157	156	221	266	263	283	319	379	401
CMW25434	*C. larium*	*Styrax benzoin*	Indonesia	GT33	203	194	218	234	M	310	422	476	135	130	177	278	431	160	157	156	221	266	263	283	N	379	401
CMW11436	*C. polychroma*	*Syzygium aromaticum*	Indonesia	GT34	209	194	234	226	294	334	401	444	126	139	182	278	431	157	153	188	229	266	307	264	306	355	389
CMW11424	*C. polychroma*	*Syzygium aromaticum*	Indonesia	GT35	209	194	234	226	294	M	401	444	126	139	182	278	431	157	153	188	229	266	307	264	N	355	389
CERC2458	*C. collisensis*	*Cunninghamia lanceolata*	FuJian	GT36	209	200	220	234	N	310	404	444	135	150	177	278	431	171	142	156	227	266	269	283	310	379	397
CERC2459	*C. collisensis*	*Cunninghamia lanceolata*	FuJian	GT37	209	200	220	234	N	310	404	444	135	150	177	278	431	171	142	156	227	266	269	283	M	379	397
CERC2466	*C. collisensis*	*Cunninghamia lanceolata*	FuJian	GT38	209	200	220	234	N	310	404	444	135	162	177	278	407	171	142	156	227	266	269	283	N	379	397

CERC2467	*C. collisensis*	*Cunninghamia lanceolata*	FuJian	GT38	209	200	220	234	N	310	404	444	135	162	177	278	407	171	142	156	227	266	269	283	N	379	397
CMW23809	*C. polyconidia*	*Acacia mearnsii*	South Africa	GT39	201	218	252	250	300	325	412	450	135	211	216	291	405	157	175	180	261	266	316	M	306	379	397
CMW23818	*C. polyconidia*	*Acacia mearnsii*	South Africa	GT40	201	218	252	250	300	325	412	450	135	211	216	291	405	157	175	180	261	266	316	M	310	379	397
CMW38543	*C. ficicola*	*Ficus carica*	Japan	GT41	201	191	231	238	273	320	407	460	138	127	172	278	455	157	160	165	N	270	287	280	303	355	397
CMW38544	*C. ficicola*	*Ficus carica*	Japan	GT41	201	191	231	238	273	320	407	460	138	127	172	278	455	157	160	165	N	270	287	280	303	355	397
CMW29120	*C. corymbiicola*	*Corymbia variegata*	Australia		M	M	M	M	270	M	M	M	135	M	M	M	M	157	M	M	261	266	M	M	310	M	397
CMW29349	*C. corymbiicola*	*Eucalyptus pilularis*	Australia		M	M	M	M	270	M	M	M	135	M	M	M	M	157	M	M	261	266	M	M	310	M	397

[1] N = Missing data

[2] M = Multiple Allele

[3] Identified as *C. changhui* in this study

Supplementary Table 2 Microsatellite summary statistics, including allele frequencies and private alleles of *Ceratocystis* species in Asian-Astralian Clade recovered from 23 microsatellite markers

Locus	Allele size	*C. cercfabiensis* N=40	*C. changhui* N=37	*C. uchidae* N=2	*C. atrox* N=2	*C. piriliformis* N=2	*C. obpyriformis* N=2	*C. larium* N=2	*C. polychroma* N=2	*C. collisensis* N=4	*C. polyconidia* N=2	*C. ficicola* N=2
AF2	192				1.000	0.500	1.000					
	201										1.000	1.000
	203	0.150						1.000				
	206	0.850				0.500						
	209								1.000	1.000		
	219[a]			**1.000**								
	220[a]		**0.378**									
	223[a]		**0.459**									
	232[a]		**0.162**									
AF3	191[a]											**1.000**
	194	1.000	1.000	1.000	1.000	1.000	1.000	1.000	1.000			
	200[a]									**1.000**		
	218[a]										**1.000**	
AF4	218[a]							**1.000**				
	220[a]									**1.000**		
	228[a]						**1.000**					
	231				1.000	0.500						1.000
	234					0.500			1.000			
	237	0.750	0.378									
	240[a]	**0.250**										
	243[a]		**0.622**									
	249[a]			**1.000**								
	252[a]										**1.000**	
AF5	226	1.000	1.000	1.000	1.000				1.000			
	230					1.000	1.000					
	234							1.000		1.000		
	238[a]											**1.000**
	250[a]										**1.000**	
AF6	252[a]						**1.000**					

	270		1.000	1.000	1.000	1.000		0.500				
	273[a]											**1.000**
	288[a]	**0.150**										
	291[a]	**0.075**										
	294	0.725							1.000			
	300[a]										**1.000**	
	N/A	0.050						0.500		1.000		
AF7	310							1.000		1.000		
	319[a]				**1.000**							
	320[a]											**1.000**
	325[a]										**1.000**	
	328	0.950	1.000									
	329[a]			**1.000**								
	334	0.050							0.500			
	340					1.000	1.000					
	N/A								0.500			
AF9	399					1.000	1.000					
	401	0.975	1.000	1.000	1.000				1.000			
	404[a]									**1.000**		
	407[a]											**1.000**
	412[a]										**1.000**	
	422[a]							**1.000**				
	N/A	0.025										
AF11	444	0.950	1.000	1.000					1.000	1.000		
	447[a]	**0.050**										
	450					1.000	0.500				1.000	
	452				1.000		0.500					
	460[a]											**1.000**
	476[a]							**1.000**				
CAA10	126	0.900	1.000	1.000		0.500	1.000		1.000			
	129	0.075			1.000	0.500						
	135							1.000		1.000	1.000	
	138[a]											**1.000**
	N/A	0.025										
CAA38	93					1.000	1.000					
	124[a]				**1.000**							
	127[a]											**1.000**
	130[a]							**1.000**				

	136	0.975	0.622									
	139			1.000					1.000			
	143	0.025	0.378									
	150[a]									**0.500**		
	162[a]									**0.500**		
	211[a]										**1.000**	
GACA650	172[a]											**1.000**
	177					1.000	1.000	1.000		1.000		
	182	1.000	1.000	1.000					1.000			
	191[a]				**1.000**							
	216[a]										**1.000**	
AG7/AG8	278	1.000	0.838	1.000		1.000	1.000	1.000	1.000	1.000		1.000
	280[a]				**1.000**							
	291[a]										**1.000**	
	N/A		0.162									
CF13/CF14	382					1.000	1.000					
	405[a]										**1.000**	
	407				1.000					0.500		
	431	1.000	1.000					1.000	1.000	0.500		
	446[a]			**1.000**								
	455[a]											**1.000**
CF23/CF24	157	1.000	1.000	1.000	1.000	1.000	1.000		1.000		1.000	1.000
	160[a]							**1.000**				
	171[a]									**1.000**		
CAA9	140					1.000	1.000					
	142[a]									**1.000**		
	147		1.000	1.000								
	153[a]								**1.000**			
	157	0.150						1.000				
	160	0.850										1.000
	175[a]										**1.000**	
	N/A				1.000							
AAG8	156							1.000		1.000		
	159[a]					**0.500**						
	165[a]											**1.000**
	171	0.025	1.000	1.000								
	174[a]	**0.975**										
	177				1.000		1.000					

	180[a]										**1.000**	
	183[a]					**0.500**						
	188[a]								**1.000**			
CAT1	219					1.000	1.000					
	221[a]							**1.000**				
	225[a]				**1.000**							
	227[a]									**1.000**		
	229[a]								**1.000**			
	232	1.000	1.000	1.000								
	261[a]										**1.000**	
	N/A											1.000
AG1/AG2	266	1.000	1.000	1.000	1.000	1.000	1.000	1.000	1.000	1.000	1.000	
	270[a]											**1.000**
CAA80	263[a]							**1.000**				
	269[a]									**1.000**		
	280[a]				**1.000**							
	284[a]			**1.000**								
	287[a]											**1.000**
	292[a]		**0.622**									
	304	1.000	0.378			1.000	1.000					
	307[a]								**1.000**			
	316[a]										**1.000**	
CAT9X	264[a]								**1.000**			
	267		1.000	1.000		1.000						
	270	1.000			1.000		1.000					
	280[a]											**1.000**
	283							1.000		1.000		
	N/A										1.000	
CAT3K	303[a]											**1.000**
	306	0.950	0.919	1.000	1.000	1.000	1.000		0.500		0.500	
	310									0.250	0.500	
	319[a]							**0.500**				
	322[a]		**0.027**									
	N/A	0.050	0.054					0.500	0.500	0.750		
CAT1200	355	1.000	1.000	1.000	1.000				1.000			1.000
	357					1.000	1.000					
	379							1.000		1.000	1.000	
AAG9	384	0.025				1.000	1.000					

386[a]				**1.000**					
389	0.050					1.000			
392	0.900	0.919	1.000						
397	0.025	0.081					1.000	1.000	1.000
401[a]					**1.000**				

N: Sample size

N/A: Missing data

Allele size[a] and number is bold: Private allele